Table 2 Treatment-related AEs occurring at a rate >10% of the total population by dose and highest CTCAE Grade ≥2

Adverse event[a]	Afatinib dose, n						All doses ($n = 12$), n (%)
	20 mg ($n = 3$)		40 mg ($n = 3$)		50 mg ($n = 6$)		
	Grade 2	Grade 3	Grade 2	Grade 3	Grade 2	Grade 3	All grades
Diarrhoea	0	0	2	0	3	1	10 (83.3)
Dry skin	1	0	1	0	2	0	9 (75.0)
Stomatitis	0	0	1	0	1	0	7 (58.3)
Rash	1	0	3	0	2	0	7 (58.3)
Paronychia	0	0	1	0	2	0	6 (50.0)
Anorexia	0	0	0	0	1	0	5 (41.7)
Nausea	0	0	1	0	2	0	3 (25.0)
Acne	0	0	0	0	1	0	3 (25.0)
Mucosal dryness	0	0	0	0	0	0	3 (25.0)
Mucosal inflammation	0	0	0	0	2	1	3 (25.0)
Blood urine present	0	0	0	0	0	0	3 (25.0)
Weight decreased	1	0	0	0	2	0	3 (25.0)
Pharyngitis	0	0	0	0	0	0	2 (16.7)
Leucopoenia	0	0	0	0	0	0	2 (16.7)
Conjunctivitis	0	0	0	0	0	0	2 (16.7)
Epistaxis	0	0	0	0	0	0	2 (16.7)
Oropharyngeal discomfort	0	0	0	0	0	0	2 (16.7)
Vomiting	0	0	0	0	1	0	2 (16.7)
Nail disorder	0	0	0	0	1	0	2 (16.7)
Pruritus	0	0	0	0	0	0	2 (16.7)
Fatigue	0	0	0	0	0	0	2 (16.7)
Malaise	0	0	0	0	0	0	2 (16.7)

AE adverse event, *CTCAE* Common terminology criteria for adverse events

[a] Preferred terms

Response was maintained for more than 11 courses before progressive disease (see Table 3). The median number (range) of courses was 2.5 (1–18).

Pharmacokinetics

Peak plasma concentrations of afatinib were reached at 3–5 h after drug administration and subsequently declined with at least in a biphasic manner (Fig. 2). In some patients, double-peak plasma concentration–time profiles of afatinib were observed. The PK parameters of afatinib are summarized in Table 4. Median t_{max} and $t_{max,ss}$ of afatinib were approximately 3–4 h. The area under the curve $(AUC)_{0-24}$ and C_{max} values of afatinib increased with increasing doses for all doses on Day 1 and all doses except 50 mg at steady state (Table 4). The geometric mean (gMean) values of the apparent total clearance were large and ranged from 799 to 1,200 mL/min on Day 1 and from 538 to 827 mL/min on Day 28. Afatinib exhibited a high apparent volume of distribution ranging from 1,880 to 2,710 L on Day 28. The terminal half-life ($t_{1/2}$) ranged from 14.8 to 37.9 h on Day 1 and from 33.5 to 40.4 h on Day 28. The gMean values of accumulation ratios (single dose vs. steady state) based on the AUC and on C_{max} were between 1.96 and 3.97, and 1.63 and 4.41, respectively. Steady state was reached at around Day 8.

Discussion

The aim of the Phase I stage of this study was to estimate the MTD of afatinib, up to 50 mg/day, in patients with advanced NSCLC and to determine the recommended dose for Phase II evaluation. In this study, afatinib 50 mg administered as an oral, once-daily continuous dose, was well tolerated with an acceptable safety profile. Whilst DLTs occurred in three of the six patients treated with afatinib 50 mg, only one patient in treatment Course 1, the treatment course in which MTD was defined, experienced a DLT. Furthermore, no DLTs resulted in study discontinuation, and all three patients who experienced DLTs continued to receive afatinib at a lower dose.

Table 3 Profiles of patients with tumour size reduction

Age (sex)	Histology	Previous treatment	Afatinib dose (daily; mg)	Month/ courses on study	Best response of targets (%)	*EGFR/HER1* mutation status	
						Tissue	Serum
67 (f)	Squamous adenocarcinoma	1. Cisplatin + amrubicin	20	2	−14.5	NA	NA
64[a] (f)	Adenocarcinoma	1. Cisplatin + TS-1 2. Gefitinib 3. Erlotinib 4. Gefitinib	20	11	−7.7	Del 19 + T790 M	NA
57[a] (f)	Adenocarcinoma	1. Cisplatin + gemcitabine 2. Nimotuzumab	40/30	18	−24.6	NA	Wild type
61[a] (f)	Squamous cell carcinoma	1. Carboplatin + paclitaxel 2. Gefitinib 3. Erlotinib	50/40/30	3	−15.3	NA	Wild type
65[a] (m)	Adenocarcinoma	1. Cisplatin + docetaxel 2. Docetaxel 3. Gefitinib 4. Gefitinib + gemcitabine 5. Gefitinib	50/40	12	−20.8	NA	Wild type
67[a] (f)	Adenocarcinoma	1. Gefitinib 2. Carboplatin + gemcitabine 3. Erlotinib 4. TS-1	50/40	3	−2.4	NA	Del 19 + T790 M

EGFR Epidermal growth factor receptor, *HER* Human epidermal growth factor receptor, *NA* not applicable

[a] Never smoker

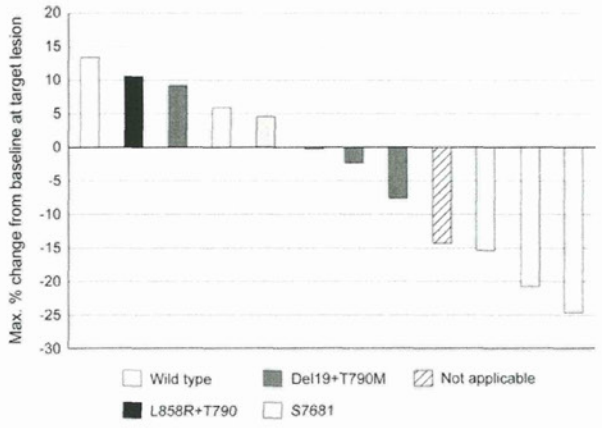

Fig. 1 Maximum tumour size reduction of individual patients by mutational status

The tolerability profile of afatinib 50 mg/day reported here in Japanese patients was similar to that previously observed in the non-Japanese population; diarrhoea and skin-related AEs were predominant and were manageable with a combination of appropriate concomitant medication and dose reduction. Therefore, continuous oral administration of afatinib at a starting dose of 50 mg once daily together with a tolerability-adapted, dose-reduction scheme and supportive care, was deemed an appropriate dosing regimen for Japanese patients in the Phase II step of this trial. Given that this patient population has already been previously treated with a reversible EGFR/HER1 TKI, dose intensity could be crucial, and the proposed dosing regimen will give these patients the opportunity of treatment with the highest possible dose for the longest duration.

Importantly, preliminary signs of efficacy were observed in this heavily pre-treated population. Although no partial or complete responses were observed, six out of 12 patients had tumour size reductions, with three achieving prolonged stable disease. This included one patient with a mutation in EGFR/HER1 exon 19 (T790 M), who remained progression-free for 11 months. This patient had previously received both gefitinib and erlotinib treatment.

Although the number of patients included in this study was limited, there appeared to be no relationship between mutation status and the maximum percentage change in target lesion from baseline or days on study. These findings support the use of afatinib as a potential novel treatment option for patients with advanced NSCLC and tumours harbouring EGFR/HER1 mutations, even after previous treatment with reversible EGFR/HER1 TKIs. The findings reported here are also in agreement with previous findings

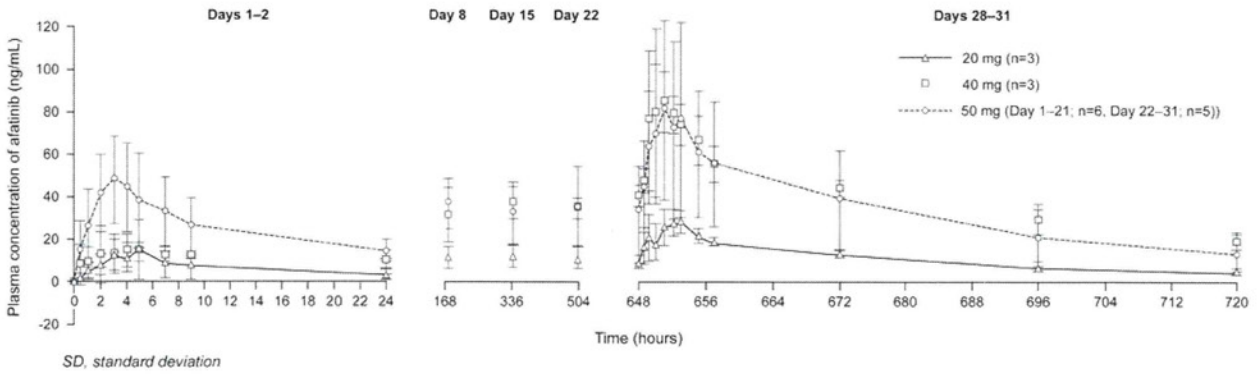

Fig. 2 Arithmetic mean (± standard deviation) plasma concentration–time profiles of afatinib after single and multiple oral administration over 28 days in Course 1

Table 4 Pharmacokinetic parameters of afatinib after multiple oral administration of afatinib 20, 40 and 50 mg once daily

Course 1	Day 1			Day 28 (steady state)		
Parameter (unit)	20 mg ($n = 3$) gMean (gCV [%])	40 mg ($n = 3$) gMean (gCV [%])	50 mg ($n = 6$) gMean (gCV [%])	20 mg ($n = 3$) gMean (gCV [%])	40 mg ($n = 3$) gMean (gCV [%])	50 mg ($n = 5$) gMean (gCV [%])
AUC_{0-24} (ng h/mL)	147 (84.5)	299 (6.0)[b]	539 (59.0)	409 (16.5)	1,240 (9.7)	1,010 (71.5)
$AUC_{0-24\ norm}$ ([ng h/mL]/mg)	7.33 (84.5)	7.47 (6.0)[b]	10.8 (59.0)	20.5 (16.5)	31.0 (9.7)	20.1 (71.5)
C_{max} (ng/mL)	12.4 (101)	18.9 (45.8)	44.4 (60.6)	26.9 (24.9)	83.3 (30.1)	66.8 (71.6)
$C_{max,\ norm}$ ([ng h/mL]/mg)	0.620 (101)	0.473 (45.8)	0.887 (60.6)	1.34 (24.9)	2.08 (30.1)	1.34 (71.6)
t^{a}_{max} (h)	3.9 (3.0–5.0)	4.1 (2.0–9.0)	3.0 (2.0–5.0)	4.0 (2.9–5.0)	3.0 (2.0–4.0)	3.0 (1.0–5.0)
$t_{½}$ (h)	21.3 (63.1)	37.9 (24.9)[b]	14.8 (20.0)	38.5 (14.4)	40.4 (11.9)	33.5 (22.2)
CL/F (mL/min)	1,200 (39.5)	799 (19.5)[b]	1,030 (55.9)	814 (16.5)	538 (9.7)	827 (71.5)
V_z/F(L)	2,200 (122.0)	2,620 (5.2)[b]	1,320 (62.8)	2,710 (30.3)	1,880 (3.8)	2,400 (80.6)

gCV geometric coefficient of variation; *gMean* geometric mean; *AUC* area under the curve; *CL* clearance

[a] median (range), [b] $n = 2$

in non-Japanese patients, in which afatinib has demonstrated activity in patients with advanced NSCLC and EGFR/HER1 mutations [16, 21]. However, it should be considered that EGFR/HER1 mutations were not identified in all patients in this study, and in three cases, mutations were identified from serum samples rather than tumour samples.

Pharmacokinetic analysis revealed that plasma concentrations of afatinib peaked at 3–4 h after administration and declined with a half-life of 30–40 h at steady state. The accumulation ratio based on the AUC values was approximately 2–4. Afatinib exhibited high apparent volume of distribution, which indicates a high tissue distribution of the drug. However, the values of the apparent volume of distribution should be interpreted with caution, as the absolute bioavailability of afatinib in humans is unknown. Steady state was considered to have been reached on Day 8 (7 days after the start of drug administration). Although dose proportionality was not evaluated statistically in this study owing to the limited number of patients, exposure of afatinib generally increased with increasing doses, and there was no obvious deviation from a dose-proportional increase in exposure. This is in agreement with findings from previous trials, which have shown no obvious deviation from dose proportionality in the dose range of 10–160 mg of afatinib [17–19, 22].

Comparison of the PK parameters obtained from previous Phase I studies in non-Japanese cancer patients suffering from advanced solid tumours [17–19, 22] to those in Japanese patients reported here revealed that the PK of afatinib in Japanese patients can be considered comparable to those in non-Japanese patients. Comparison of the individual AUC and C_{max} values of Japanese and non-Japanese patients showed that although the AUC and C_{max} values tended to be higher in Japanese patients than in non-Japanese patients at some doses, most values in Japanese were within the same range of those in non-Japanese (Fig. 3). T_{max} and $t_{1/2}$ values reported here in Japanese

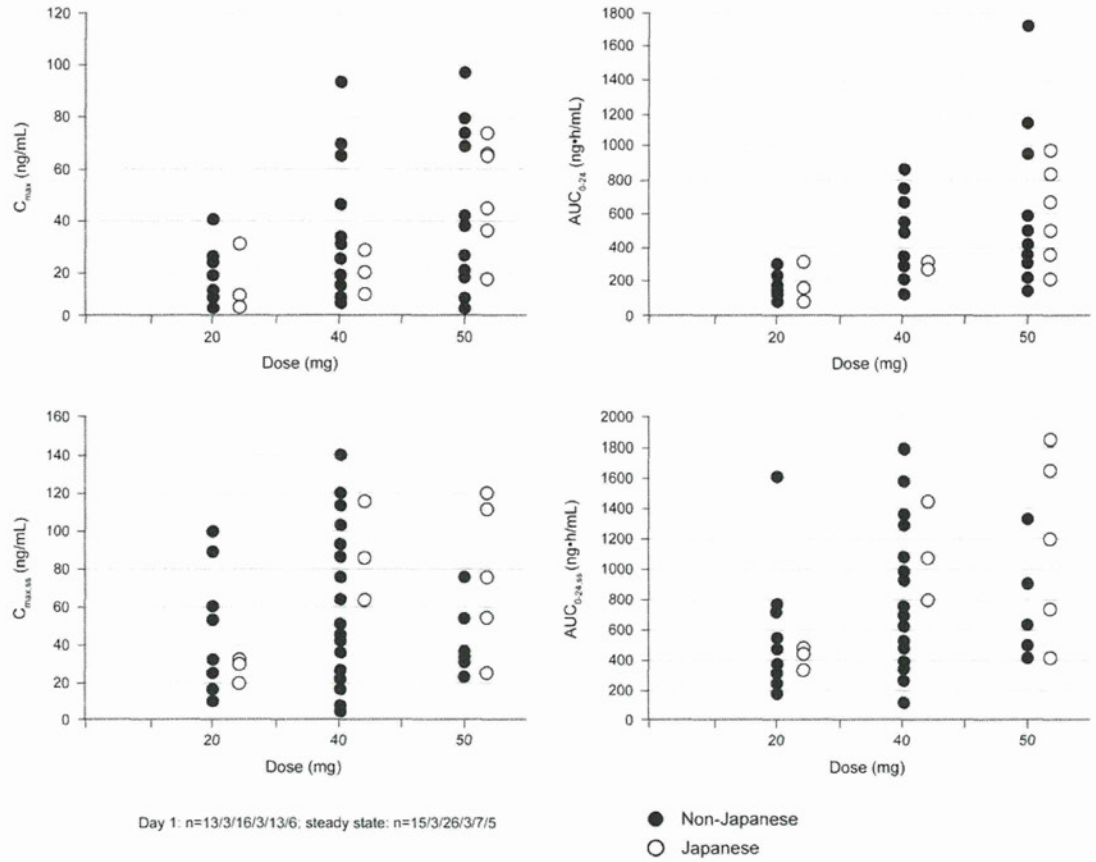

Fig. 3 Comparison of pharmacokinetic parameters between Japanese and non-Japanese patients. Comparison of pharmacokinetic parameters showed that although the area under the curve and C_{max} values tended to be higher in Japanese patients than in non-Japanese patients at some doses, most values in Japanese were within the same range of those in non-Japanese

patients were also within the same range as those in non-Japanese patients. Whilst we cannot rule out that pharmacogenomic differences between Japanese and non-Japanese patients may have an effect on the pharmacodynamic profile of afatinib, no such observations were made in this study, and the mechanism by which pharmacogenomic differences in patient populations may exert an effect on the pharmacodynamics of afatinib remains to be clearly established.

In conclusion, the recommended dose for Phase II study in Japanese patients is 50 mg/day. Further evaluation of afatinib in NSCLC patients who have been previously treated with erlotinib and/or gefitinib in the Phase II part of this trial is currently being conducted. Furthermore, a Phase III trial with afatinib in an enriched population of TKI-naïve NSCLC patients is currently ongoing.

Acknowledgments This study was supported by Boehringer Ingelheim. The authors acknowledge the editorial assistance of Ogilvy Healthworld. Boehringer Ingelheim provided financial support for this assistance.

Conflict of interest Haruyasu Murakami, Tomohide Tamura, Toshiaki Takahashi, Hiroshi Nokihara, Tateaki Naito, Yukiko Nakamura, Kazuto Nishio, Nobuyuki Yamamoto: nothing to disclose. Yoko Seki, Akiko Sarashina, Mehdi Shahidi: employee of Boehringer Ingelheim.

References

1. Winer E, Gralow J, Diller L, Karlan B, Loehrer P, Pierce L, Demetri G, Ganz P, Kramer B, Kris M, Markman M, Mayer R, Pfister D, Raghavan D, Ramsey S, Reaman G, Sandler H, Sawaya R, Schuchter L, Sweetenham J, Vahdat L, Schilsky R, Blayney D, Lichter A (2008) Clinical cancer advances 2008: major research advances in cancer treatment, prevention, and screening–a report from the American Society of Clinical Oncology. J Clin Oncol 27(5):812–826. doi:10.1200/JCO.2008.21.2134
2. Hynes NE, Lane HA (2005) ERBB receptors and cancer: the complexity of targeted inhibitors. Nat Rev Cancer 5(5):341–354. doi:10.1038/nrc1609
3. Salomon DS, Brandt R, Ciardiello F, Normanno N (1995) Epidermal growth factor-related peptides and their receptors in human malignancies. Crit Rev Oncol Hematol 19(3):183–232. doi:1040842894001441

4. Arteaga CL (2002) Epidermal growth factor receptor dependence in human tumors: more than just expression? Oncologist 7(Suppl 4):31–39
5. Johnson BE, Jackman D, Janne PA (2006) Impact of EGFR mutations on treatment of non-small cell lung cancer. Cancer Chemother Pharmacol 58(Suppl 7):5–9
6. Doroshow JH (2005) Targeting EGFR in non-small-cell lung cancer. N Engl J Med 353(2):200–202. doi:10.1056/NEJMe058113
7. Giaccone G, Rodriguez JA (2005) EGFR inhibitors: what have we learned from the treatment of lung cancer? Nat Clin Pract Oncol 2(11):554–561
8. Fukuoka M, Yano S, Giaccone G, Tamura T, Nakagawa K, Douillard JY, Nishiwaki Y, Vansteenkiste J, Kudoh S, Rischin D, Eek R, Horai T, Noda K, Takata I, Smit E, Averbuch S, Macleod A, Feyereislova A, Dong RP, Baselga J (2003) Multi-institutional randomized phase II trial of gefitinib for previously treated patients with advanced non-small-cell lung cancer (The IDEAL 1 Trial). J Clin Oncol 21(12):2237–2246
9. Paez JG, Janne PA, Lee JC, Tracy S, Greulich H, Gabriel S, Herman P, Kaye FJ, Lindeman N, Boggon TJ, Naoki K, Sasaki H, Fujii Y, Eck MJ, Sellers WR, Johnson BE, Meyerson M (2004) EGFR mutations in lung cancer: correlation with clinical response to gefitinib therapy. Science 304(5676):1497–1500
10. Shepherd FA, Rodrigues Pereira J, Ciuleanu T, Tan EH, Hirsh V, Thongprasert S, Campos D, Maoleekoonpiroj S, Smylie M, Martins R, van Kooten M, Dediu M, Findlay B, Tu D, Johnston D, Bezjak A, Clark G, Santabarbara P, Seymour L (2005) Erlotinib in previously treated non-small-cell lung cancer. N Engl J Med 353(2):123–132. doi:10.1056/NEJMoa050753
11. Engelman JA, Janne PA (2008) Mechanisms of acquired resistance to epidermal growth factor receptor tyrosine kinase inhibitors in non-small cell lung cancer. Clin Cancer Res 14(10):2895–2899. doi:10.1158/1078-0432.CCR-07-2248
12. Turke AB, Zejnullahu K, Wu YL, Song Y, Dias-Santagata D, Lifshits E, Toschi L, Rogers A, Mok T, Sequist L, Lindeman NI, Murphy C, Akhavanfard S, Yeap BY, Xiao Y, Capelletti M, Iafrate AJ, Lee C, Christensen JG, Engelman JA, Janne PA (2010) Preexistence and clonal selection of MET amplification in EGFR mutant NSCLC. Cancer Cell 17(1):77–88. doi: 10.1016/j.ccr.2009.11.022
13. Maheswaran S, Sequist LV, Nagrath S, Ulkus L, Brannigan B, Collura CV, Inserra E, Diederichs S, Iafrate AJ, Bell DW, Digumarthy S, Muzikansky A, Irimia D, Settleman J, Tompkins RG, Lynch TJ, Toner M, Haber DA (2008) Detection of mutations in EGFR in circulating lung-cancer cells. N Engl J Med 359(4):366–377. doi:10.1056/NEJMoa0800668
14. Li D, Ambrogio L, Shimamura T, Kubo S, Takahashi M, Chirieac LR, Padera RF, Shapiro GI, Baum A, Himmelsbach F, Rettig WJ, Meyerson M, Solca F, Greulich H, Wong KK (2008) BIBW2992, an irreversible EGFR/HER2 inhibitor highly effective in preclinical lung cancer models. Oncogene 27(34):4702–4711. doi:10.1038/onc.2008.109
15. Plummer R, Vidal L, Li L, Shaw H, Perrett R, Shahidi M, Amelsberg A, Temple G, Calvert H, de Bono J (2006) Phase I study of BIBW 2992, an oral irreversible dual EGFR/HER2 inhibitor, showing activity in tumours with mutated EGFR. Eur J Cancer Suppl 4(12):174
16. Yang C-H, Shih J, Su W, Hsia T, Sequist LV, Chang G, Calvo R, Cong XJ, Shahidi M, Miller VA (2010) A phase II study of BIBW 2992 in patients with adenocarcinoma of the lung and activating EGFR/HER1 mutations (LUX-LUNG2). Ann Oncol 21(Suppl8):viii122–viii161 (abstract 367PD)
17. Agus DB, Terlizzi E, Stopfer P, Amelsberg A, Gordon MS (2006) A phase I dose escalation study of BIBW 2992, an irreversible dual EGFR/HER2 receptor tyrosine kinase inhibitor, in a continuous schedule in patients with advanced solid tumours. J Clin Oncol 24(18S):2074
18. Eskens FA, Mom CH, Planting AS, Gietema JA, Amelsberg A, Huisman H, van Doorn L, Burger H, Stopfer P, Verweij J, de Vries EG (2008) A phase I dose escalation study of BIBW 2992, an irreversible dual inhibitor of epidermal growth factor receptor 1 (EGFR) and 2 (HER2) tyrosine kinase in a 2-week on, 2-week off schedule in patients with advanced solid tumours. Br J Cancer 98(1):80–85. doi:10.1038/sj.bjc.6604108
19. Lewis N, Marshall J, Amelsberg A, Cohen RB, Stopfer P, Hwang J, Malik S (2006) A phase I dose escalation study of BIBW 2992, an irreversible dual EGFR/HER2 receptor tyrosine kinase inhibitor, in a 3 week on 1 week off schedule in patients with advanced solid tumors. ASCO Meet Abstr 24 (18_suppl):3091
20. Yap TA, Vidal L, Adam J, Stephens P, Spicer J, Shaw H, Ang J, Temple G, Bell S, Shahidi M, Uttenreuther-Fischer M, Stopfer P, Futreal A, Calvert H, de Bono J, Plummer R (2010) Phase I trial of the irrevisible ErbB1 (EGFR) and ErbB2 (HER2) kinase inhibitor BIBW 2992 in patients with advanced solid tumours. J Clin Oncol 28(25):3965–3972
21. Plummer R, Vidal L, Perrett R, Spicer J, Stopfer P, Shahidi M, Temple G, Futreal A, Calvert H, de Bono J (2007) A Phase I and pharmacokinetic (PK) study of BIBW 2992, an oral irreversible dual EGFR/HER2 inhibitor. Eur J Cancer Suppl 5(4):108
22. Spicer J, Calvert H, Vidal L, Azribi F, Perrett R, Shahidi M, Temple G, Futreal A, De Bono J, Plummer R (2007) Activity of BIBW2992, an oral irreversible dual EGFR/HER2 inhibitor, in non-small cell lung cancer (NSCLC) with mutated EGFR. J Thorac Oncol 2(8):S410

Cancer Science
The official journal of the Japanese Cancer Association

Integrated analysis of whole genome exon array and array-comparative genomic hybridization in gastric and colorectal cancer cells

Kazuyuki Furuta,[1,2] Tokuzo Arao,[1] Kazuko Sakai,[1] Hideharu Kimura,[1] Tomoyuki Nagai,[1] Daisuke Tamura,[1] Keiichi Aomatsu,[1] Kanae Kudo,[1] Hiroyasu Kaneda,[1] Yoshihiko Fujita,[1] Kazuko Matsumoto,[1] Yasuhide Yamada,[3] Kazuyoshi Yanagihara,[4] Masaru Sekijima[2] and Kazuto Nishio[1,5]

[1]Department of Genome Biology, Kinki University Faculty of Medicine, Osaka; [2]Advanced Medical Science Research Center, Mitsubishi Chemical Medience, Tokyo; [3]Department of Medical Oncology, National Cancer Center Hospital, Tokyo; [4]Department of Life Sciences, Yasuda Women's University, Hiroshima, Japan

(Received April 19, 2011/Revised October 11, 2011/Accepted October 17, 2011/Accepted manuscript online October 28, 2011)

Whole genome-scale integrated analyses of exon array and array-comparative genomic hybridization are expected to enable the identification of unknown genetic features of cancer cells. Here, we evaluated this approach in 22 gastric and colorectal cancer cell lines, focusing on protein kinase genes and genes belonging to the cadherin–catenin family. Regarding alternative splicing patterns, several cancer cell lines predominantly expressed isoform 1 of protein kinase A catalytic subunit beta (*PRKACB*). Paired gastric cancer specimens demonstrated that isoform 1 of *PRKACB* was a novel cancer-related variant transcript in gastric cancers. In addition, the exon array analysis clearly identified exon 3 or exon 3–4 skipping in *catenin beta 1*, a short intron insertion with exon 9 skipping in *CDH1*, and a deletional transcript of *CDH13*. These abnormal transcripts were shown to have arisen from small genomic deletions. Meanwhile, an integrated analysis of 11 gastric cancer cell lines revealed that four cell lines amplified fibroblast growth factor receptor 2, with truncated forms observed in two of the cell lines. Gene amplification, and not the truncated form, was found to determine the sensitivity to a fibroblast growth factor receptor inhibitor, indicating that our cell line panel might be useful for cell-based evaluations of specific inhibitors. Using an integrated analysis, we identified several abnormal transcripts and genomic alterations in gastric and colorectal cancer cells. Our approach might enable genetic changes to be identified more efficiently, and the present results warrant further investigation using clinical samples and integrated analyses. (*Cancer Sci*, doi: 10.1111/j.1349-7006.2011.02132.x, 2011)

Recent advancements in the field of array technology over the past several years have enabled alternative splicing and abnormal transcripts to be explored at the whole genome level. Accordingly, the identification of cancer-related transcripts has been intensively investigated at the whole genome level in lung cancer, glioblastoma, thymic tumors and colorectal cancer using exon arrays, yielding novel splice variants, hyper-splicing signatures and overexpressed variants.[1–4] In contrast, whole genome array-comparative genomic hybridization (array-CGH) has enabled a higher resolution and probe density and is expected to make possible the identification of relatively small genomic copy number changes caused by gene amplifications and deletions that were previously undetectable. The array-CGH tool is also producing promising data for cancer research and the diagnosis, classification, and outcome prediction of different malignancies.[5]

In relation to abnormal transcripts caused by genomic changes, mutations and small genomic deletions can disrupt or create splice sites, change other consensus sequences, or affect splicing silencers or enhancers, such as *ATM* and *BRCA1*.[6] The detection of these transcripts containing exon-level abnormalities is thought to be difficult using conventional methods, and unknown genetic changes might exist. Therefore, we hypothesized that the use of only an exon analysis or an array-CGH might be insufficient, and that a simultaneous analysis might contribute to the further identification of abnormal transcripts in cancer cells.

In the present study, we performed a whole genome exon array and array-CGH analysis in gastric and colorectal cancer cells with the objective of identifying abnormal transcripts at the exon level.

Materials and Methods

Cell lines and cultures and sample preparations. The method used in this section is described in Data S1.

Clinical samples. The endoscopic biopsy samples were obtained from gastric cancer and paired non-cancerous lesions of gastric mucosa. The samples were immediately placed in an RNA stabilization solution (Isogen, Nippongene, Tokyo, Japan) and stored at −80°C. This analysis was approved by the Institutional Review Board of the National Cancer Center Hospital, and written informed consent was obtained from all the patients.

Exon array. Two micrograms of total RNA was used as the starting material. rRNA was first removed using the RiboMinus Human/Mouse Transcriptome Isolation Kit (Invitrogen, Carlsbad, CA, USA) and cDNA synthesis was performed using the GeneChip WT cDNA Synthesis Kit (Affymetrix, Santa Clara, CA, USA). The cDNA was fragmented and labeled with biotin using the GeneChip WT Terminal Labeling Kit (Affymetrix). Biotinylated targets were hybridized onto a GeneChip Human Exon 1.0 ST Array (Affymetrix) according to the manufacturer's instructions. The array was washed and stained in Fluidics Station 450 (Affymetrix) and scanned to generate a CEL file using the GeneChip Scanner 3000 (Affymetrix) and GeneChip Operating Software version 1.4.

Array-based comparative genomic hybridization. The Genome-wide Human SNP Array 6.0 (Affymetrix) was used to perform array-CGH on genomic DNA from each of the colorectal cancer cell lines and MKN74 according to the manufacturer's instructions. The GeneChip Human Mapping 250K Nsp Array (Affymetrix) was used to perform array-CGH on genomic DNA from each of the gastric cancer cell lines, with the exception of MKN74, according to the manufacturer's instructions. The method is described in detail in Data S1.

[5]To whom correspondence should be addressed. E-mail: knishio@med.kindai.ac.jp

doi: 10.1111/j.1349-7006.2011.02132.x

RT-PCR, sequencing and colony formation assay. The method used in this section is described in Data S1.

***In vitro* growth inhibition assay.** The growth-inhibitory effects of the fibroblast growth factor receptor (FGFR) inhibitor PD173074 (Sigma-Aldrich, St. Louis, MO, USA) were examined using an MTT assay, as previously described.[7]

siRNA study. The methods used in this section have been previously described.[8]

Statistical analysis. All exon array data were analyzed using Partek Genomic Suite 6.4 software (Partek, St. Louis, MO, USA). The robust multi-array average algorithm was used for the exon-level intensity analysis. Exon-level data were filtered to include only those probe sets that were included within the ''Core Meta-Probeset.'' The software calculated the differences between the cancer cell lines and the normal samples for each probe set on the transcript. The alt-splice score was the minimum *P*-value from the *Z*-test of each probe set's difference against the remaining probe sets. A low Alt-splice score indicates that at least one probe set behaved differently from the rest. The Alt-Splice score was used to screen the transcript variants. In the array-CGH analysis, sample-specific copy number changes were analyzed using Partek Genomic Suite 6.4 software (Partek) and Affymetrix Genotyping Console ver.3.0.2 (Affymetrix) for the 40 samples of Human HapMap JPT.

Results

Cβ1 isoform of protein kinase A catalytic subunit beta is a novel cancer-related variant transcript. To evaluate the use of an integrated analysis involving an exon array and an array-CGH, we applied a focused-gene approach against cancer-related and relatively annotated genes, including 480 protein kinase genes and 68 cadherin–catenin genes in gastric and colorectal cancer cell lines.

Cyclic adenosine monophosphate-dependent protein kinase is a signaling molecule that is important for a variety of cellular functions.[9] Alternatively spliced transcript variants encoding distinct isoforms have been found in protein kinase cAMP-dependent catalytic beta (PRKACB).[10,11] Interestingly, an exon analysis showed that isoform 1 of *PRKACB* (Cβ1 isoform) are frequently expressed in gastric and colorectal cancer cell lines, but not in normal mucosa (Fig. 1A). Among colorectal cancers, WiDr, LoVo and normal colonic mucosa predominantly expressed the Cβ2 isoform, whereas the CaR-1, DLD-1, CoCM-1, RCM-1, OUMS-23 and COLO320 DM cells expressed the Cβ1 isoform. Meanwhile, the HCC56, COLO201 and SW837 cell lines expressed very low levels. Similar expression patterns were observed in gastric cancer and normal gastric mucosa. RT-PCR confirmed these results (Fig. S1A). The RT-PCR study and

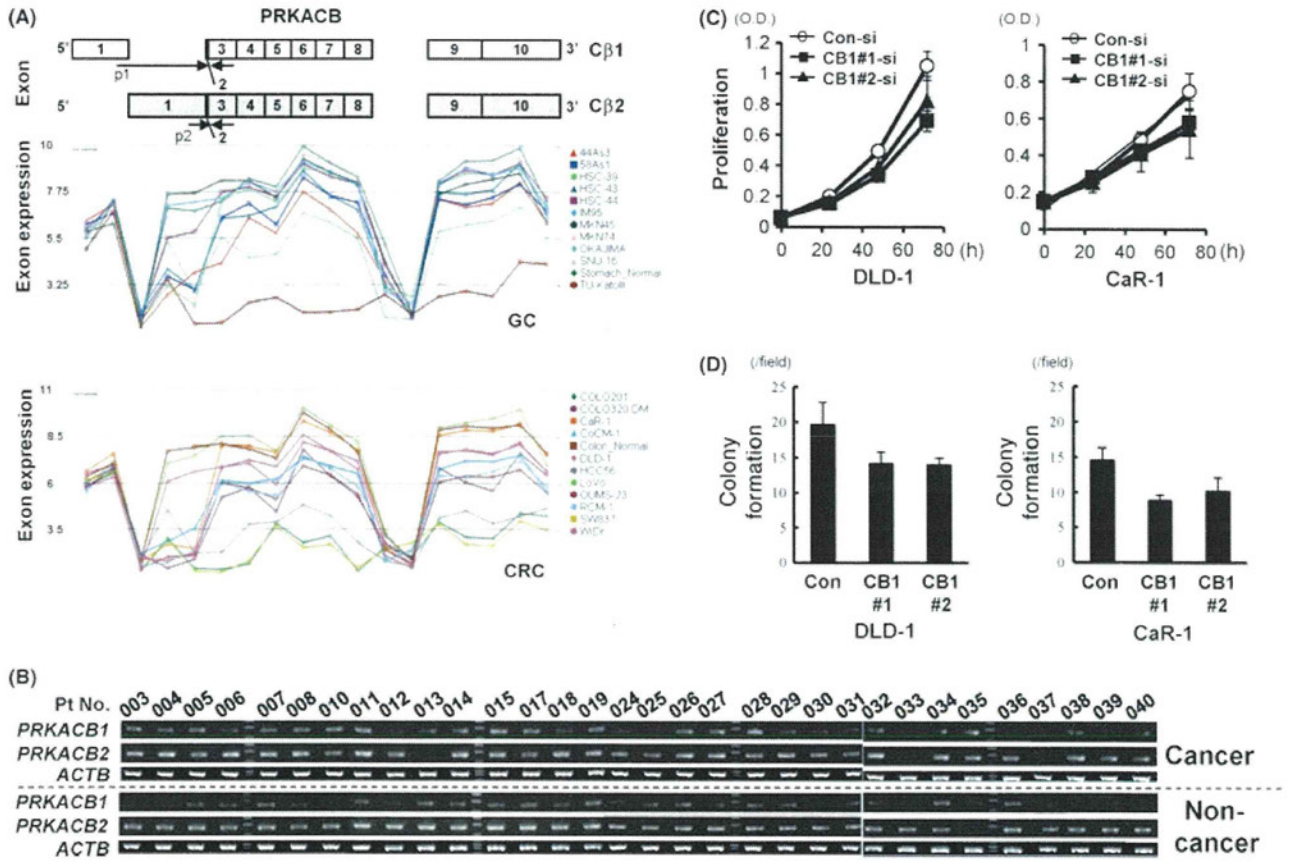

Fig. 1. Cancer-related alternative splicing variants of protein kinase cAMP-dependent catalytic beta (*PRKACB*). (A) Exon array analysis showing the exon level mRNA expressions of *PRKACB* in 22 gastric and colorectal cancer cell lines and one gastric and one colorectal normal mucosa specimen. The log2-transformed values indicate the expression levels of each exon. The schematic diagram in the upper panel shows each exon of *PRKACB* (Cβ1 and Cβ2 isoforms). Note that normal gastric and colonic tissues and some cancer cell lines predominantly expressed the Cβ2 isoform, but several cancer cell lines predominantly expressed the Cβ1 isoform. p1–2: primer set. GC: 11 gastric cancer cell lines and one normal gastric mucosa specimen. CRC: 11 colorectal cancer cell lines and one normal colonic mucosa specimen. Cβ1, Cβ2: isoforms of *PRKACB*. (B) RT-PCR analysis for Cβ1 and Cβ2 isoforms of *PRKACB* in 32 paired gastric cancer and non-cancerous gastric mucosa specimens. (C) Knockdown of Cβ1 isoform of *PRKACB* using specific siRNA for Cβ1 and resulting cellular proliferation in DLD-1 and CaR-1 cell lines. Two different sequences of Cβ1-targeting siRNA (CB1#1 and CB1#2; 10 nM each) were used. Con-si, control siRNA. (D) Evaluation of colony formation in siRNA-treated DLD-1 and CaR-1 cell lines.

doi: 10.1111/j.1349-7006.2011.02132.x

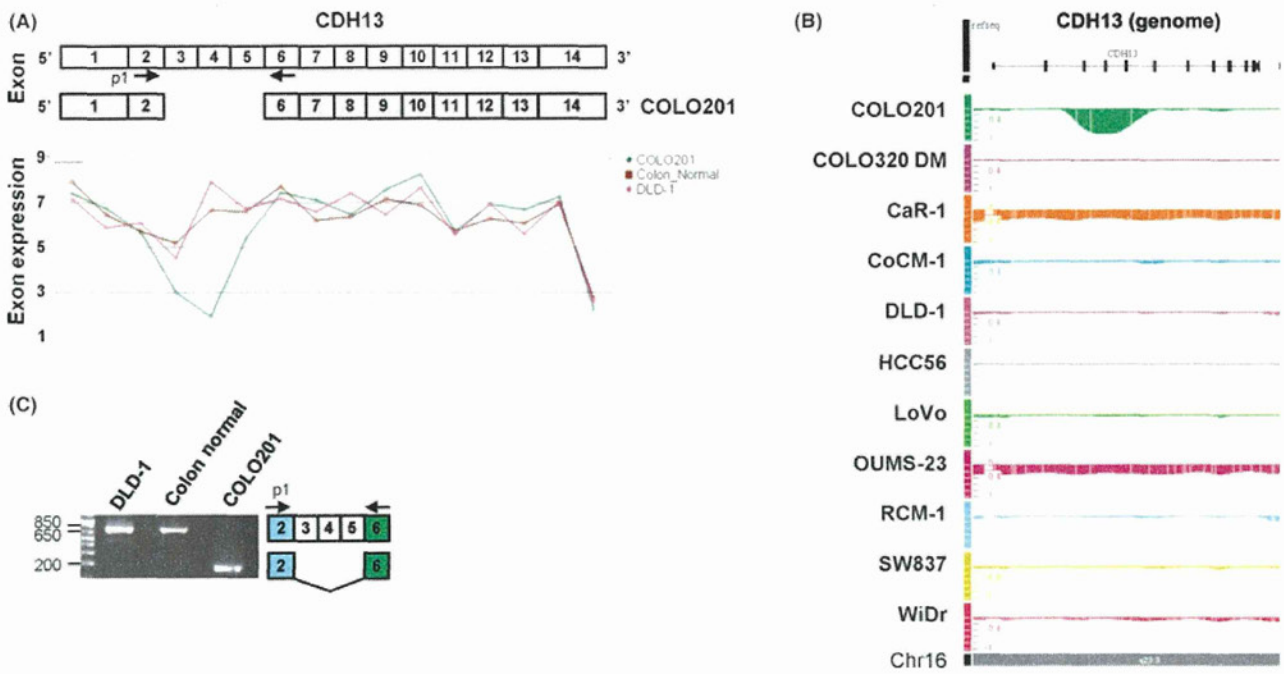

Fig. 2. Truncated transcripts of *CDH13* caused by small genomic deletion. (A) Exon array analysis showing the exon level mRNA expressions of *CDH13* in COLO201 (lacking exons 3–5), DLD-1 and a normal colonic mucosa specimen. The log2-transformed values indicate the expression levels of each exon. The schematic diagram in the upper panel shows each exon of CDH13. p1: primer set. (B) Array-comparative genomic hybridization analysis for *CDH13* locus in 11 colorectal cancer cell lines. The loss of genomic copy number is shown as bars extending toward the minus side of the baseline. (C) Detection of truncated mutant transcripts using RT-PCR for COLO201 (lacking exon 3–5), DLD-1 (normal) and normal colonic mucosa (normal). The schematic diagram shows each exon of *CDH13*. p1: primer set.

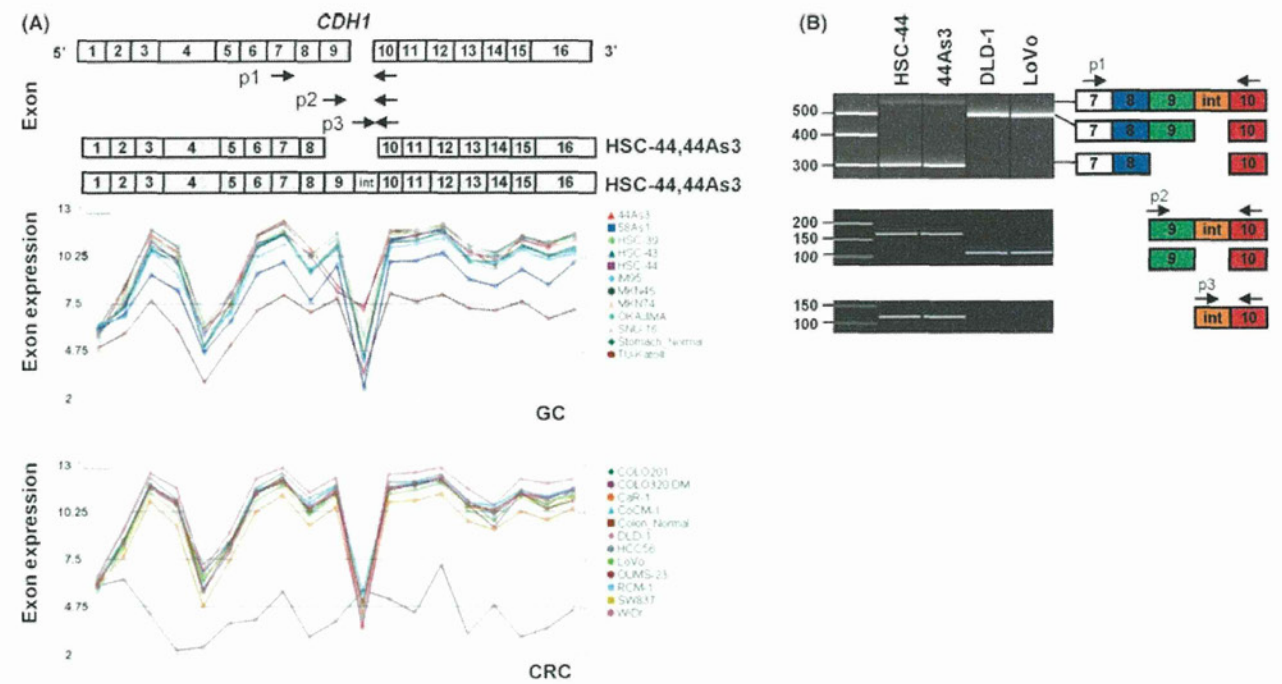

Fig. 3. Identification of mutant transcripts with a short intron insertion and exon skipping in *CDH1/E-cadherin*. (A) Exon array analysis showing the exon level mRNA expressions of *CDH1* in 22 gastric and colorectal cancer cell lines and one gastric and one colorectal normal mucosa specimen. The log2-transformed values indicate the expression levels of each exon. The schematic diagram in the upper panel shows each exon of *CDH1*. p1–3: primer set. GC: 11 gastric cancer cell lines and one normal gastric mucosa specimen. CRC: 11 colorectal cancer cell lines and one normal colonic mucosa specimen. Note that exon 9 expression was downregulated and intron expression was observed in HSC-44 and 44As3 cells. int, intron. (B) Detection of mutant transcripts using RT-PCR and microfluidics-based electrophoresis for HSC-44 and 44As3 (lacking exon 9 or short intron insertion) and other control cell lines. The schematic diagram shows each exon of *CDH1*. p1–3: primer set.

the densitometrical analysis confirmed that the Cβ1 isoform was predominantly expressed in 32 gastric cancer specimens, compared with paired non-cancerous mucosa specimens in RT-PCR (P = 0.0012, Figs 1B and S1B). The expression of the Cβ2 isoform of *PRKACB* was not significantly different between the cancer and paired gastric mucosa specimens (P = 0.21). These results demonstrated that the Cβ1 isoform of *PRKACB* is a novel cancer-specific variant transcript in gastric cancer. We examined the biological functions of the Cβ1 isoform of *PRKACB* using specific siRNA for Cβ1 in DLD-1 and CaR-1 cell lines. The knockdown of the Cβ1 isoform significantly reduced cellular proliferation in both the DLD-1 and CaR-1 cell lines (Fig. 1C). In addition, a colony assay revealed that the knockdown of the Cβ1 isoform significantly reduced colony formation in both cell lines (Fig. 1D). These results suggest that the Cβ1 isoform, which is overexpressed in cancer cells, is involved in cellular proliferation in cancer cells. Because a recent study has demonstrated that specific *PRKACB* isoforms can properly recruit activated $p75^{NTR}$ to lipid rafts and determine $p75^{NTR}$ bioactivity, these different isoforms of *PRKACB* in cancer and normal cells might occur during carcinogenesis and might perform specific biological functions.[12]

Identification of truncated transcripts caused by small genomic deletions. Alterations of the cadherin–catenin cell adhesion system are considered to be a cause of gastric and colorectal cancers; therefore, we analyzed genes involved in this system. We found a novel truncated transcript of the *CDH13/cadherin 13/H-cadherin* gene. An exon analysis of *CDH13* showed that the expression levels of exons 3–5 were extremely downregulated in COLO201 cells compared with other cell lines (Fig. 2A). Next, using array-CGH analysis, we evaluated the *CDH13* locus and identified a small genomic deletion (approximately 0.4 Mbp) involving exons 3–5 in COLO201 cells (Fig. 2B). RT-PCR and sequencing confirmed the truncated transcript (Figs 2C and S2). Genomic PCR of exon 4 of *CDH13* revealed a heterozygous deletion (data not shown).

Mutations in the *CDH1/E-cadherin* gene are a well-documented cause of hereditary diffuse gastric cancer.[13] The exon analysis easily detected both the downregulation of exon 9 and an intron insertion in HSC-44 and its subline 44As3 (Fig. 3A). RT-PCR and sequencing confirmed these abnormal transcripts (Figs 3B and S3). Genomic PCR showed a 10-base deletion at the exon–intron boundary of the *CDH1* gene (exon 9 and intron 9) in HSC-44 and 44As3 (data not shown). Meanwhile, the exon analysis clearly demonstrated the presence of a truncated *catenin beta 1* (*CTNNB1*) transcript lacking exons 3–4 as a result of a small genomic deletion in HSC-39 cells (Fig. 4A). In addition, we found another type of truncated *CTNNB1* transcript lacking exon 3 in HCC56. RT-PCR confirmed the deleted transcript (Fig. 4B). Genomic PCR demonstrated that the deletion of these transcripts was caused by a homozygous genomic deletion (data not shown). These results indicated that this integration analysis could detect exon-level mRNA abnormalities involving genomic deletions.

Whole genome analysis of alternatively spliced transcript variants and gene copy number profiles. Next, we screened for cancer-specific spliced transcripts in each cancer cell line and compared the results with those for a normal mucosa sample using exon array data obtained at the whole genome level (Data

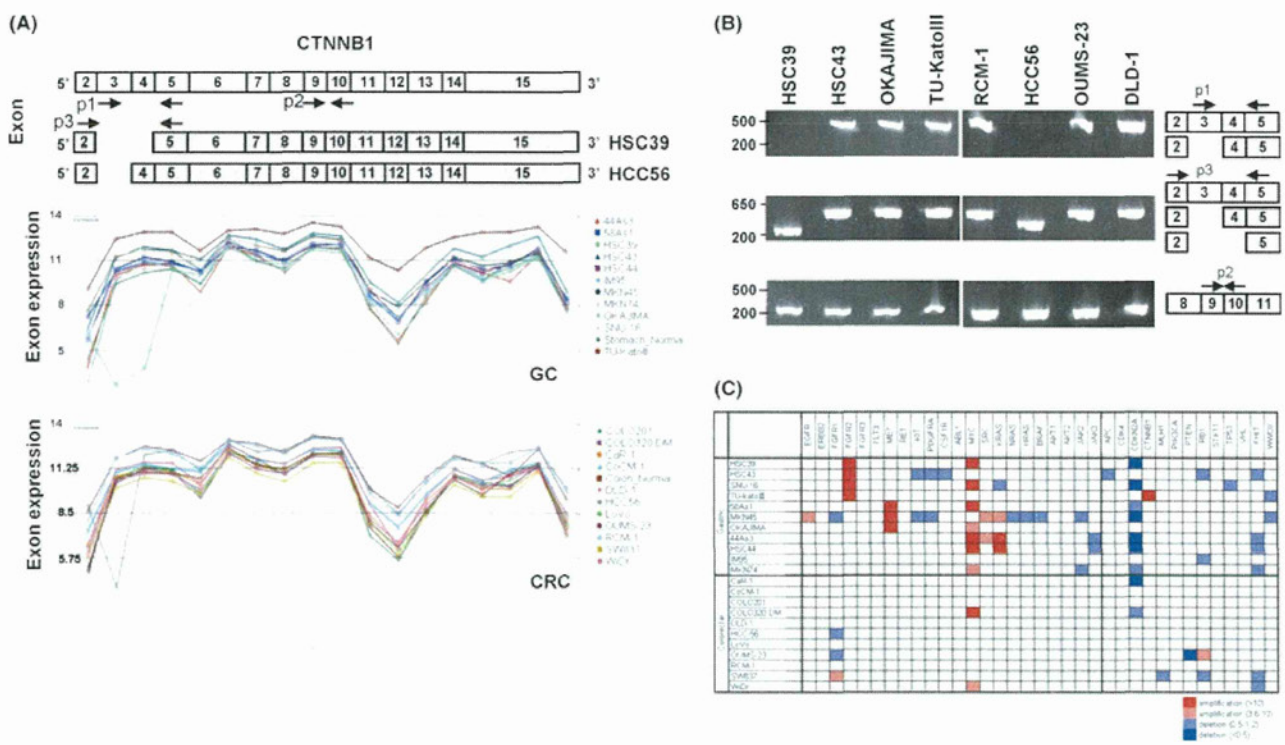

Fig. 4. Identification of truncated mutant transcripts of *CTNNB1*. (A) Exon array analysis showing the exon level mRNA expression of *CTNNB1* in 22 gastric and colorectal cancer cell lines and one gastric and one colorectal normal mucosa specimen. The log2-transformed values indicate the expression levels of each exon. The schematic diagram in the upper panel shows each exon of *CTNNB1*. p1–3: primer set. GC: 11 gastric cancer cell lines and one normal gastric mucosa specimen. CRC: 11 colorectal cancer cell lines and one normal colonic mucosa specimen. (B) Detection of truncated mutant transcripts using RT-PCR for HSC-39 (lacking exons 3–4), HCC56 (lacking exon 3) and other control cell lines. p2 primer were used as a positive control. The schematic diagram shows each exon of *CTNNB1*. p1–3: primer set. (C) DNA copy number analysis for major oncogenes and tumor suppressor genes in 11 gastric and 11 colorectal cancer cell lines using array-comparative genomic hybridization analysis. Gene amplification (≥10 copies and 10–3.6 copies) and deletion (≤0.5 copies and 1.2–0.5 copies) are shown by the indicated colors.

doi: 10.1111/j.1349-7006.2011.02132.x

Table 1. List of overlapping genes with altered exon expressions and copy numbers

Gene symbol	Name	RefSeq	Transcript ID	No. of cell lines	Alt-splice score	Copy number	Cancer
FGFR2	Fibroblast growth factor receptor 2	NM_022970	3310041	3	0.00011	Amp	GC
KIAA1797	KIAA1797	NM_017794	3164601	3	0.00053	Del	GC
ASAP1	ArfGAP with SH3 domain, ankyrin repeat and PH domain 1	NM_018482	3153428	2	0.00006	Amp	GC
ATP8A1	ATPase, type 8A, member 1	NM_006095	2767378	2	0.00021	Del	GC
CNDP2	CNDP dipeptidase 2	NM_018235	3793760	2	0.00051	Del	GC
DENND4C	DENN/MADD domain containing 4C	NM_017925	3164221	2	0.00041	Del	GC
GAS6	Growth arrest-specific 6	NM_000820	3502829	2	0.00047	Amp	GC
ITPR2	Inositol 1,4,5-trisphosphate receptor, type 2	NM_002223	3448152	2	0.00019	Amp/Del	GC
NFRKB	Nuclear factor related to kappaB binding protein	NM_006165	3398076	2	0.00040	Amp/Del	GC
PCDHGC5	Protocadherin gamma subfamily C, 5	NM_018929	2832533	2	0.00012	Del	GC
PCM1	Pericentriolar material 1	NM_006197	3087813	2	0.00011	Del	GC
PEX1	Peroxisomal biogenesis factor 1	NM_000466	3061191	2	0.00025	Amp	GC
PHLPP	PH domain and leucine rich repeat protein phosphatase 1	NM_194449	3791482	2	0.00024	Del	GC
PIGN	Phosphatidylinositol glycan anchor biosynthesis, class N	NM_176787	3811086	2	0.00009	Del	GC
RGS12	Regulator of G-protein signaling 12	NM_198227	2716025	2	0.00045	Del	GC
SHROOM3	Shroom family member 3	NM_020859	2732068	2	0.00021	Del	GC
SMARCA2	SMARC, subfamily a, member 2	NM_003070	3159946	2	0.00027	Del	GC
SPG7	Spastic paraplegia 7	NM_199367	3674048	2	0.00019	Del	GC
TAF4	TAF4 RNA polymerase II	NM_003185	3912718	2	0.00071	Amp/Del	GC
TLN1	Talin 1	NM_006289	3204744	2	0.00055	Amp/Del	GC
UBA6	Ubiquitin-like modifier activating enzyme 6	NM_018227	2771718	2	0.00023	Del	GC
WDR7	WD repeat domain 7	NM_052834	3789442	2	0.00039	Del	GC
KIAA1967	KIAA1967	NM021174	3089597	3	0.00029	Del	CRC
MYCBP2	MYC binding protein 2	NM_015057	3518496	2	0.00045	Amp/Del	CRC
TH1L	TH1-like (Drosophila)	NM_198976	3891278	2	0.00071	Amp	CRC
WDR7	WD repeat domain 7	NM_052834	3789442	2	0.00045	Del	CRC

No. of cell lines, overlapping cell lines with altered exon expressions (Alt-Splice Score < 0.001) and copy numbers (amplification, >3.6 copies and deletion, <1.2 copies). Amp, gene amplification; CRC, colorectal cancer; Del, gene deletion; GC, gastric cancer.

S2 and S3). Fourteen and ten transcripts were identified as recurrently altered genes observed in more than six cell lines among the 11 gastric cancer cell lines and the 11 colorectal cancer cell lines, respectively (Data S4). The whole genome gene copy number profiles were also examined for 22 cancer cell lines (Data S5, Figs S4 and S5). In addition, we analyzed and identified overlapping genes between the results of an exon array (Alt-Splice Score) and an array-CGH (copy number changes) analysis at the whole genome level. The identified genes are listed according to the number of overlapping cell lines and are shown in Table 1. In the list, the *FGFR2* gene tops the list of overlapping genes, suggesting that the results of the whole genome level approach were consistent with those of the focused-gene approach. Interestingly, the second-ranked gene, *KIAA1797*, was deleted in approximately 30% of the genomic region and expressed a truncated transcript, because the *KIAA1797* gene locus was located at the end of the deleted region, including *CDKN2A*, in SNU-16 cells (data not shown). However, some genes identified using the focused-gene approach, including *CDH1*, *CDH13* and *CTNNB1*, were not selected using the whole genome level analysis. These results indicate that an integrated analysis of the exon array and an array-CGH analysis might be better performed using both a whole genome level approach and a focused-gene approach.

Gene copy number profile using array-comparative genomic hybridization analysis. We evaluated changes in the gene copy number, including gene amplification/deletion and chromosomal gain/loss, in a set of 35 definitive oncogenes and tumor suppressor genes by referring to a previous report.[14] The gene copy number profiles for a panel of 22 gastric and colorectal cancer cell lines are shown in Figure 4(C). A gain in the copy number was frequently observed in *MYC* (41%, 9/22), *FGFR2* (18%, 4/22), *MET* (14%, 3/22), *KRAS* (14%, 3/22) and *SRC* (9%, 2/22). Meanwhile, a loss of copy number was observed in *CDKN2A* (41%, 9/22), *FHIT* (27%, 6/22), *FGFR1* (14%, 3/22) and *RB1* (14%, 3/22). A loss of copy number for *KIT* and *PDGFRA*, located side-by-side on chromosome 4q12, was unexpectedly observed in two gastric cancer cell lines (HSC-43 and MKN45). Interestingly, *MET* and *FGFR2* were exclusively amplified only in gastric cancers. The results also suggested that copy number changes occur more frequently in gastric cancers than in colorectal cancers.

Fibroblast growth factor receptor 2 amplification, C-terminus truncation and sensitivity to fibroblast growth factor receptor inhibitor. We previously reported that FGFR2-amplified gastric cancer cell lines were markedly sensitive to a small molecule inhibitor with a kinase inhibitory effect on FGFR, and some of the *FGFR2*-amplified cell lines dominantly expressed a C-terminus truncated *FGFR2*.[15] In this study, we evaluated the truncated-*FGFR2* transcripts using an exon array analysis (Fig. 5A). The exon array demonstrated that HSC-39, HSC-43, SNU-16 and TU-KATOIII cells overexpressed *FGFR2*, and amplification was also confirmed using an array-CGH (Fig. 5B). Notably, a C-terminus truncated form of *FGFR2* lacking exon 17 was observed dominantly in HSC-43 and partially in TU-KATOIII. RT-PCR for exons 16–17 and exons 2–3 (control) confirmed these results (Fig. 5C). Array-CGH data also showed that the FGFR2-amplicon included the following genes in HSC-39 (*FGFR2*), HSC-43 (*BRWD2*, *FGFR2* and *ATE1*), SNU-16 (*PPAPDC1A*, *BRWD2*, *FGFR2* and *ATE1*) and

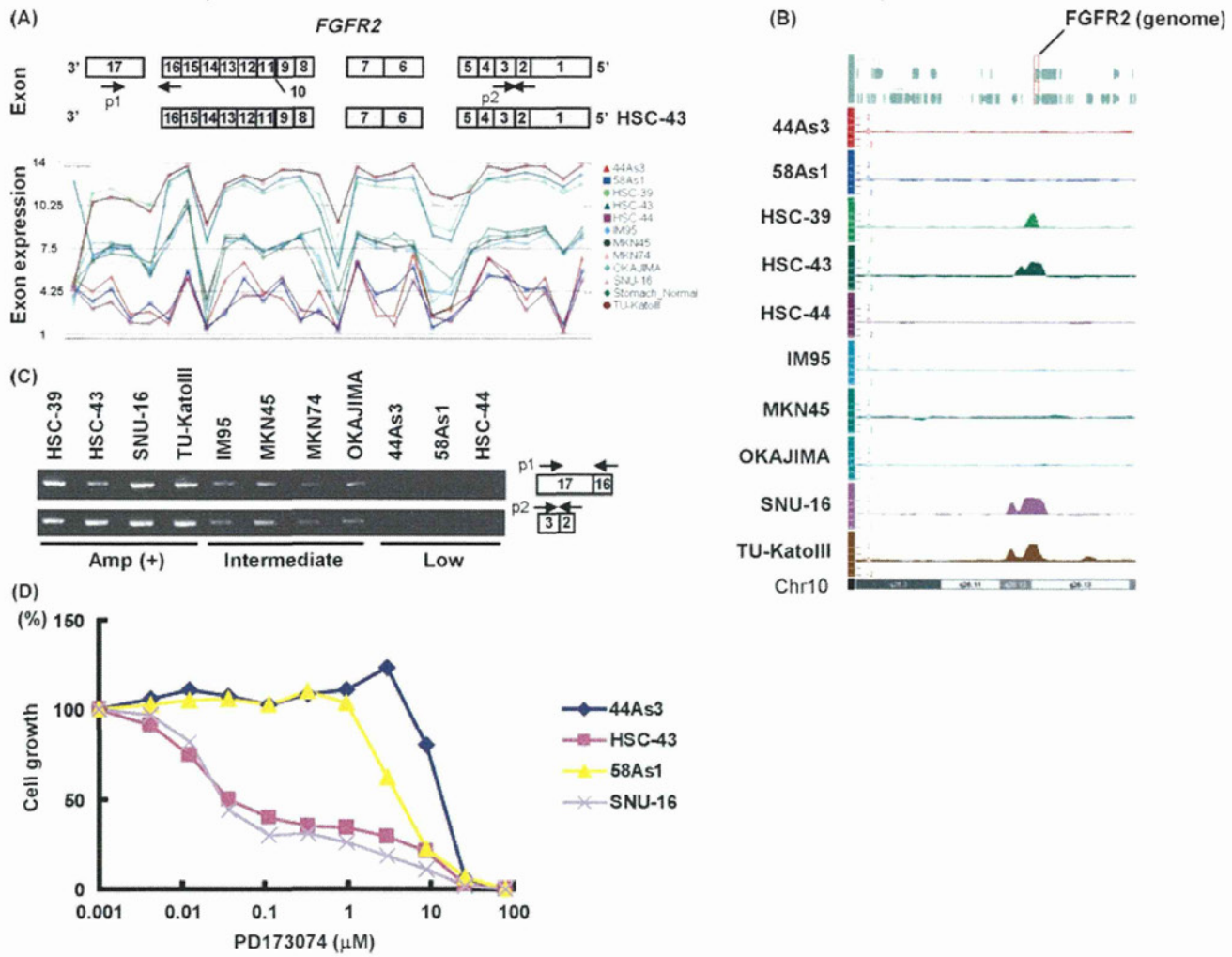

Fig. 5. *FGFR2* amplification and marked sensitivity to fibroblast growth factor receptor (FGFR) tyrosine kinase inhibitor in gastric cancer cell lines. (A) Exon array analysis showing the exon level mRNA expression of *FGFR2* in 11 gastric and cancer cell lines and one gastric normal mucosa specimen. The log2-transformed values indicate the expression levels of each exon. The schematic diagram in the upper panel shows each exon of *FGFR2*. Note that *FGFR2* is overexpressed in HSC-39, HSC-43, SNU-16 and TU-KATOIII cells (log2 scale), and a C-terminus truncation of *FGFR2* is observed in HSC-43 and partially in TU-KATOIII. p1–2: primer set. (B) Array-comparative genomic hybridization analysis of *FGFR2* locus in 10 gastric cancer cell lines. A gain of genomic copy number is shown as a bar extending toward the plus side of the baseline (HSC-39, HSC-43, SNU-16 and TU-KATOIII cells). (C) The mRNA expression levels of *FGFR2* were detected using RT-PCR and the following primer (p1, C-terminus region; p2, common region). (D) Growth inhibitory effect of the FGFR tyrosine kinase inhibitor PD173074 in *FGFR2*-amplified (HSC-43 and SNU-16) and non-amplified (44As3 and 58As1) gastric cancer cell lines.

TU-KATOIII (*PPAPDC1A*, *BRWD2* and *FGFR2*). As expected, only FGFR2-amplified cell lines, which dominantly express the truncated form (HSC-43) or the wild-type form (SNU-16), exhibited a remarkable sensitivity (approximately 100-fold) to the FGFR tyrosine kinase inhibitor PD173074, indicating that the major determinant of sensitivity to the FGFR inhibitor was *FGFR2* amplification, and not truncation, in the case of *FGFR2* (Fig. 5D).

These results for *FGFR2* amplification and drug sensitivity suggested that an integrated analysis involving an exon array and array-CGH is useful for the rapid and efficient identification of factors that determine sensitivity to molecular-targeted drugs and for evaluating abnormal transcripts that are amplified.

Discussion

Normal gastric and colonic tissues expressed the Cβ2 isoform of *PRKACB*; however, we found that gastric cancer specimens predominantly expressed the Cβ1 isoform (Fig. 1). The large difference in the expressions of variants between gastric cancer cells and paired non-cancerous gastric mucosa suggests that the predominant expression of the Cβ1 isoform increases during carcinogenesis or is involved in the malignant phenotype. Because these cancer-specific alternative splice variants might be useful therapeutic targets in cancer treatment, the significance of cancer-related isoforms of *PRKACB* warrants further biological investigation.

We found that *CTNNB1*, *CDH13* and *CDH1* expressed mutated transcripts that were caused by small genomic deletions in gastric and colorectal cancer cells. *CDH13* is considered to be a tumor suppressor gene, and its expression is downregulated by the hypermethylation of the promoter region in breast, ovarian and lung cancers.[16] COLO201 cells expressed novel mutated transcripts lacking exons 3–5 as a result of a small genomic deletion (approximately 0.4 Mb, Fig. 2A). Because this deletion was too small to detect using an array-CGH in a standard

doi: 10.1111/j.1349-7006.2011.02132.x

manner, it would have been overlooked if the exon expression data had not been available (Fig. 2A,B). Collectively, an integrated analysis involving a whole genome exon array and an array-CGH might be a promising and efficient approach for identifying mutated transcripts on a whole genome scale, even when the mutated transcripts are produced by relatively small and exon-level genomic deletions in cancer cells.

Recent successful clinical developments of molecular-targeted drugs, largely targeting constitutively activated oncogenes such as tyrosine kinases, show that mechanisms enabling a gain-of-function in oncogenes could be promising therapeutic targets.[17] In this study, drug sensitivity and gene amplification were highly correlated (Fig. 5), indicating that cell-based evaluations using a genetically well-characterized cell line panel for uncharacterized compounds might be useful for identifying factors that determine sensitivity.

In conclusion, we found several abnormal transcripts and genomic alterations in gastric and colorectal cancer cells using an integrated analysis involving a whole genome exon array and array-CGH. Our approach might enable discoveries in cancer genetics to be made more efficiently than with the use of conventional methods and warrants further investigation involving integrated analyses of clinical samples. Our results also suggest that the combination of a whole genome level approach and a focused-gene approach might be an effective strategy.

Acknowledgments

This study was supported by the Third-Term Comprehensive 10-Year Strategy for Cancer Control and a Grant-in-Aid for Cancer Research from the Ministry of Health, Labour and Welfare (22-9 and 22-15). We thank Miss Tomoko Kitayama for her technical assistance.

Disclosure Statement

All authors declare no financial support or relationship that may pose conflict of interest.

References

1 Xi L, Feber A, Gupta V *et al.* Whole genome exon arrays identify differential expression of alternatively spliced, cancer-related genes in lung cancer. *Nucleic Acids Res* 2008; **36**: 6535–47.
2 Cheung HC, Baggerly KA, Tsavachidis S *et al.* Global analysis of aberrant pre-mRNA splicing in glioblastoma using exon expression arrays. *BMC Genomics* 2008; **9**: 216.
3 Soreq L, Gilboa-Geffen A, Berrih-Aknin S *et al.* Identifying alternative hyper-splicing signatures in MG-thymoma by exon arrays. *PLoS ONE* 2008; **3**: e2392.
4 Gardina PJ, Clark TA, Shimada B *et al.* Alternative splicing and differential gene expression in colon cancer detected by a whole genome exon array. *BMC Genomics* 2006; **7**: 325.
5 Shinawi M, Cheung SW. The array CGH and its clinical applications. *Drug Discov Today* 2008; **13**: 760–70.
6 Pajares MJ, Ezponda T, Catena R, Calvo A, Pio R, Montuenga LM. Alternative splicing: an emerging topic in molecular and clinical oncology. *Lancet Oncol* 2007; **8**: 349–57.
7 Arao T, Fukumoto H, Takeda M, Tamura T, Saijo N, Nishio K. Small in-frame deletion in the epidermal growth factor receptor as a target for ZD6474. *Cancer Res* 2004; **64**: 9101–4.
8 Kaneda H, Arao T, Tanaka K *et al.* FOXQ1 is overexpressed in colorectal cancer and enhances tumorigenicity and tumor growth. *Cancer Res* 2010; **70**: 2053–63.
9 Gerits N, Kostenko S, Shiryaev A, Johannessen M, Moens U. Relations between the mitogen-activated protein kinase and the cAMP-dependent protein kinase pathways: comradeship and hostility. *Cell Signal* 2008; **20**: 1592–607.
10 Ørstavik S, Reinton N, Frengen E, Langeland BT, Jahnsen T, Skålhegg BS. Identification of novel splice variants of the human catalytic subunit Cbeta of cAMP-dependent protein kinase. *Eur J Biochem* 2001; **268**: 5066–73.
11 Murray AJ. Pharmacological PKA inhibition: all may not be what it seems. *Sci Signal* 2008; **1**: re4.
12 Higuchi H, Yamashita T, Yoshikawa H, Tohyama M. PKA phosphorylates the p75 receptor and regulates its localization to lipid rafts. *EMBO J* 2003; **22**: 1790–800.
13 Brooks-Wilson AR, Kaurah P, Suriano G *et al.* Germline E-cadherin mutations in hereditary diffuse gastric cancer: assessment of 42 new families and review of genetic screening criteria. *J Med Genet* 2004; **41**: 508–17.
14 MacConaill LE, Campbell CD, Kehoe SM *et al.* Profiling critical cancer gene mutations in clinical tumor samples. *PLoS ONE* 2009; **4**: e7887.
15 Takeda M, Arao T, Yokote H *et al.* AZD2171 shows potent antitumor activity against gastric cancer over-expressing fibroblast growth factor receptor 2/keratinocyte growth factor receptor. *Clin Cancer Res* 2007; **13**: 3051–7.
16 Kim JS, Han J, Shim YM, Park J, Kim DH. Aberrant methylation of H-cadherin (CDH13) promoter is associated with tumor progression in primary non-small cell lung carcinoma. *Cancer* 2005; **104**: 1825–33.
17 Cowan-Jacob SW, Möbitz H, Fabbro D. Structural biology contributions to tyrosine kinase drug discovery. *Curr Opin Cell Biol* 2009; **21**: 280–7.

Supporting Information

Data S1. Materials and methods in detail.

Data S2. Exon array analysis for gastric cancer cell lines.

Data S3. Exon array analysis for colorectal cancer cell lines.

Data S4. Exon array analysis for recurrently altered genes.

Data S5. Array-comparative genomic hybridization analysis for gastric and colorectal cancer cell lines.

Fig. S1. Expression levels of *PRKACB1* isoform.

Fig. S2. Sequencing analysis for *CDH13* transcripts.

Fig. S3. Sequencing analysis for *CDH1* transcripts.

Fig. S4. Comparative genomic hybridization (CGH) analysis for gastric cancer cell lines.

Fig. S5. Comparative genomic hybridization (CGH) analysis for colorectal cancer cell lines.

Lung Cancer 76 (2012) 362–367

Contents lists available at SciVerse ScienceDirect

Lung Cancer

journal homepage: www.elsevier.com/locate/lungcan

Randomized phase II study of first-line carboplatin-paclitaxel with or without bevacizumab in Japanese patients with advanced non-squamous non-small-cell lung cancer

Seiji Niho[a,*], Hideo Kunitoh[b], Hiroshi Nokihara[b], Takeshi Horai[c], Yukito Ichinose[d], Toyoaki Hida[e], Nobuyuki Yamamoto[f], Masaaki Kawahara[g], Tetsu Shinkai[h], Kazuhiko Nakagawa[i], Kaoru Matsui[j], Shunichi Negoro[k], Akira Yokoyama[l], Shinzoh Kudoh[m], Katsuyuki Kiura[n], Kiyoshi Mori[o], Hiroaki Okamoto[p], Hiroshi Sakai[q], Koji Takeda[r], Soichiro Yokota[s], Nagahiro Saijo[i], Masahiro Fukuoka[i], JO19907 Study Group

[a] *National Cancer Center Hospital East, Chiba, Japan*
[b] *National Cancer Center Hospital, Tokyo, Japan*
[c] *Cancer Institute Hospital, Japanese Foundation for Cancer Research, Tokyo, Japan*
[d] *National Kyushu Cancer Center, Fukuoka, Japan*
[e] *Aichi Cancer Center Hospital, Nagoya, Japan*
[f] *Shizuoka Cancer Center, Naga-izumi, Japan*
[g] *Kinki-Chuo Chest Medical Center, Osaka, Japan*
[h] *National Shikoku Cancer Center, Matsuyama, Japan*
[i] *Kinki University School of Medicine, Osaka, Japan*
[j] *Osaka Prefectural Medical Center for Respiratory and Allergic Disease, Habikino, Japan*
[k] *Hyogo Cancer Center, Akashi, Japan*
[l] *Niigata Cancer Center Hospital, Niigata, Japan*
[m] *Osaka City University Medical School, Osaka, Japan*
[n] *Okayama University Graduate School of Medicine, Dentistry and Pharmaceutical Science, Okayama, Japan*
[o] *Tochigi Cancer Center, Utsunomiya, Japan*
[p] *Yokohama Municipal Citizen's Hospital, Yokohama, Japan*
[q] *Saitama Cancer Center, Saitama, Japan*
[r] *Osaka City General Hospital, Osaka, Japan*
[s] *Toneyama National Hospital, Osaka, Japan*

ARTICLE INFO

Article history:
Received 27 October 2011
Received in revised form
16 December 2011
Accepted 18 December 2011

Keywords:
Non-small cell lung cancer
Bevacizumab
Carboplatin
Paclitaxel
Advanced lung cancer
Chemonaïve

ABSTRACT

Purpose: This multicenter, randomized, open-label, phase II study (JO19907) compared the efficacy and safety of first-line carboplatin-paclitaxel (CP) alone with bevacizumab-CP in Japanese patients with advanced non-squamous non-small-cell lung cancer (NSCLC).
Methods: Chemonaïve patients with stage IIIB, IV or recurrent non-squamous NSCLC were eligible for participation. Patients were randomly assigned in a 2:1 ratio to receive bevacizumab-CP or CP alone. Chemotherapy was repeated for up to 6 cycles or until disease progression or unacceptable toxicity. Bevacizumab recipients who completed ≥3 cycles of chemotherapy could continue bevacizumab as monotherapy until disease progression or unacceptable toxicity. The primary endpoint was progression-free survival (PFS).
Results: After confirming the tolerability of bevacizumab-CP in a small number of patients, 180 patients were recruited, of whom 121 were assigned to bevacizumab-CP and 59 to CP alone. Hazard ratio (HR) for PFS was 0.61 with bevacizumab-CP versus CP alone ($p = 0.0090$; median 6.9 versus 5.9 months). Objective response rate was significantly higher with bevacizumab-CP than with CP alone (60.7% versus 31.0%; $p = 0.0013$). Median overall survival was >22 months in both treatment groups (HR 0.99; $p = 0.9526$). No new safety signals were detected.

* Corresponding author at: Department of Thoracic Oncology, National Cancer Center Hospital East, 6-5-1 Kashiwanoha, Kashiwa, Chiba, 277-8577 Japan. Tel.: +81 4 7133 1111; fax: +81 4 7131 9960.
E-mail address: siniho@east.ncc.go.jp (S. Niho).

0169-5002/$ – see front matter
doi:10.1016/j.lungcan.2011.12.005

Conclusion: Study JO19907 met its primary endpoint, demonstrating that the addition of bevacizumab to first-line CP significantly improves PFS in Japanese patients with advanced non-squamous NSCLC. This prolonged PFS by bevacizumab did not translate into OS benefit with the extremely longer underlying survival compared to historical data. No new safety signals were identified in this population. (Japan Pharmaceutical Information Center [JAPIC] registration number: CTI-060338).

1. Introduction

Bevacizumab is a humanized monoclonal antibody that specifically targets vascular endothelial growth factor, inhibiting angiogenesis, thereby impeding tumor growth and survival. In trials that recruited mainly Western populations, bevacizumab given with first-line chemotherapy and continued as monotherapy until disease progression has been shown to be effective in patients with non-squamous non-small-cell lung cancer (NSCLC). A phase III trial (E4599) performed in patients with non-squamous NSCLC, which was conducted primarily in the USA, demonstrated that the addition of bevacizumab (15 mg/kg) to first-line carboplatin-paclitaxel (CP) significantly prolonged overall survival (OS; hazard ratio [HR] 0.79; $p = 0.003$) [1]. That pivotal trial was of particular clinical significance given that bevacizumab extended median OS beyond the historic 8-month benchmark achieved with conventional platinum-based chemotherapy [2]. In a second phase III trial (AVAiL), which was conducted principally in European patients with non-squamous NSCLC, addition of bevacizumab (7.5 or 15 mg/kg) to another commonly-used first-line chemotherapy regimen (cisplatin-gemcitabine) significantly improved progression-free survival (PFS [HR] 0.75; $p = 0.003$) [3].

While bevacizumab has been robustly evaluated in Western populations, its efficacy and tolerability have not been investigated in Japanese patients with NSCLC. It is important that targeted agents that are established in Western patients are also studied in Japanese patients, as ethnic differences may influence response to treatment and safety profiles. This has been highlighted in several recent studies reporting that Asian patients may respond differently to targeted agents compared with Western patients, for example, epidermal growth factor receptor inhibitors (EGFR-TKIs) such as erlotinib and gefitinib have been associated with improved responses in Asian patients with NSCLC [4,5]. Especially, in Japanese patients with NSCLC the frequency of EGFR mutations is higher (40% or more) compared with Western populations, and in Japanese population with EGFR mutations, gefitinib showed improved PFS compared to conventional chemotherapies in the first line treatment setting [6,7]. In addition, prospective comparisons of CP therapy between three randomized phase III studies have suggested that chemonaïve Japanese patients with NSCLC have prolonged OS and PFS, with this chemotherapy than US patients [6]. This may be due to differences in genotypic distribution of genes involved in paclitaxel disposition or DNA damage repair [8], and further highlights the importance of evaluating cancer treatments in different ethnic populations.

We report the final results of the randomized phase II study JO19907 in Japan, the only study in Asia which compared the efficacy and safety of first-line CP with or without bevacizumab in patients with advanced non-squamous NSCLC.

2. Patients and methods

JO19907 was a multicenter, randomized, open-label, phase II study conducted at 19 sites in Japan. The protocol was approved by the institutional review boards of all participating centers and was conducted in accordance with the Declaration of Helsinki and Guideline for Good Clinical Practices. All patients provided written informed consent prior to any study-specific procedures being performed.

2.1. Patients

Eligible patients were aged 20–74 years and had histologically or cytologically documented stage IIIB with pleural and/or pericardial effusion and/or pleural dissemination, IV or recurrent non-squamous NSCLC. Patients were also required to have: measurable lesions as defined by Response Evaluation Criteria in Solid Tumors (RECIST 1.0);[9] an Eastern Cooperative Oncology Group Performance Status (ECOG PS) of 0 or 1; life expectancy of ≥3 months; and adequate bone marrow, hepatic, and renal function. Key exclusion criteria were: prior chemotherapy for NSCLC; central nervous system metastases or spinal cord compression; a tumor invading major blood vessels or with cavitation; hemoptysis (≥2.5 mL per event); history of coagulation disorders or therapeutic anticoagulation; uncontrolled hypertension; or history of a symptomatic lung disorder.

2.2. Study design

The study was conducted in two steps. Step 1 was performed to evaluate the tolerability of bevacizumab-CP in Japanese patients. In this step, six patients received bevacizumab-CP intravenously on day 1 of a 21-day cycle. Carboplatin was administered at a dose calculated to produce an area-under-the-curve (AUC) of 6 mg/(mL min), paclitaxel was administered at a dose of 200 mg/m^2 and bevacizumab at a dose of 15 mg/kg. AEs were assessed based on the National Cancer Institute Common Terminology Criteria for Adverse Events (NCI-CTCAE) v3.0. Transition to step 2 of the trial was possible if no more than two patients presented during the first treatment cycle with grade 4 hematologic toxicities or grade ≥3 non-hematologic toxicities.

In step 2, eligible patients were randomly assigned in a 2:1 ratio to receive bevacizumab-CP or CP alone with no placebo for bevacizumab. Randomization was performed centrally and patients were stratified according to disease stage (IIIB, IV, or recurrent), ECOG PS, and gender. All treatments were administered on day 1 of a 21-day cycle according to the regimens described in step 1. Chemotherapy was repeated every 21 days for a total of 6 cycles unless there was evidence of disease progression or unacceptable toxicity. In the absence of disease progression, patients who were treated with bevacizumab and who completed at least 3 cycles of chemotherapy could continue with bevacizumab monotherapy until disease progression or unacceptable toxicity.

2.3. Efficacy and safety assessments

After the baseline evaluation, tumor lesions were evaluated every 6 weeks for the first 18 weeks, thereafter every 9 weeks until evidence of disease progression. Responses were assessed by computed tomography, magnetic resonance imaging, or x-ray using RECIST 1.0. PFS, the primary endpoint of this study, and responses were assessed by an Independent Review Committee in a blind manner. AEs were monitored throughout the study and graded using NCI-CTCAE v3.0.

2.4. Pharmacokinetic assessments

Blood samples were collected prior to and 1 h after every infusion of bevacizumab until the sixth cycle from patients randomized to bevacizumab-CP. The pharmacokinetic profile of bevacizumab was characterized using non-linear regression by fitting a one-compartment model to bevacizumab serum concentrations (WinNonlin v4.1; Pharsight, St. Louis, MO). The following parameters were estimated: clearance (CL); volume of distribution (Vd); half-life ($t_{½}$), AUC from zero to infinity (AUC_{inf}) and mean residence time (MRT).

2.5. Statistical analysis

PFS was defined as the time from randomization to first documented disease progression or death, whichever occurred first. Secondary endpoints included OS, objective response rate (ORR), time to response, duration of response, disease control rate (DCR; sum of complete responses plus partial responses plus stable disease), pharmacokinetics, and safety. Efficacy analyses were performed on eligible patients who underwent tumor evaluation at least once after the baseline assessment. Safety analyses were performed on all patients who received at least one dose of study treatment.

On the basis of the PFS benefit reported in E4599 (HR 0.66; $p < 0.001$) [1], it was estimated that addition of bevacizumab to CP would reduce the risk of disease progression by 35%. Given this assumption, an HR point-estimate for PFS of 0.8 or better could be taken to indicate a treatment difference similar to that observed in E4599. The study was designed to have an 86.8% conditional probability to detect an effect on PFS similar to that found in E4599. The PFS analysis was planned after 130 events; therefore, to allow for event and drop-out rates, the trial enrolled 180 patients.

Time-to-event distributions were estimated by the Kaplan–Meier method. Between-treatment differences at each time-to-event endpoint were tested with a two-sided stratified log-rank test adjusted with the stratification factors used for randomization. HRs were calculated by Cox proportional-hazards methods adjusted with the stratification factors for randomization. Exploratory forward stepwise regression analyses with the use of the Cox model were performed to adjust for treatment effect on PFS.

3. Results

Patients were enrolled between April 2007 and March 2008. The clinical data cut-off dates were November 2008 for analysis of the primary endpoint (PFS), February 2009 for analysis of the safety and February 2010 for analysis of the secondary endpoint (OS). As planned, six patients were enrolled in step 1 of the study. None of the predefined toxicities were reported in these six patients.

3.1. Patient characteristics

A total of 180 patients were recruited to step 2 of the study: 121 were assigned to bevacizumab-CP (Fig. 1). Three patients were excluded from the safety and efficacy analyses as they did not begin treatment due to ineligibility confirmed, clinically unacceptable high total dose of carboplatin calculated, or withdrawn consent, and a further two patients were excluded from the efficacy analysis because they did not have measurable disease. Table 1 shows selected demographic and baseline characteristics of all randomly assigned patients. The two groups were well balanced at baseline.

Table 1
Summary of baseline patient characteristics and demographics.

Variable	CP ($n = 59$)	Bevacizumab-CP ($n = 121$)
Median age, years (range)	60 (38–73)	61 (34–74)
Age <65 years, *n* (%)	40 (68%)	73 (60%)
Age ≥65 years, *n* (%)	19 (32%)	48 (40%)
Gender, *n* (%)		
Male	38 (64%)	77 (64%)
Female	21 (36%)	44 (36%)
ECOG PS, *n* (%)		
0	29 (49%)	62 (51%)
1	30 (51%)	59 (49%)
Tumor histology, *n* (%)		
Adenocarcinoma	55 (93%)	111 (92%)
Large cell carcinoma	2 (3%)	2 (2%)
Other	2 (3%)	8 (7%)
Stage, *n* (%)		
IIIB	12 (20%)	28 (23%)
IV	42 (71%)	83 (69%)
Recurrent	5 (8%)	10 (8%)
Smoking status, *n* (%)		
Never smoker	19 (32%)	38 (31%)
Current or past smoker	40 (68%)	83 (69%)

CP, carboplatin plus paclitaxel; ECOG, Eastern Cooperative Oncology Group; PS, performance status.

3.2. Treatment

The median number of chemotherapy cycles was 6 in the bevacizumab-CP group and 4.5 in the CP group. After initial bevacizumab-CP treatment of between 3 and 6 cycles, 72 patients (60.5%) received bevacizumab monotherapy for a median of 6 cycles (range 1–25).

3.3. Efficacy analysis

The HR for PFS with bevacizumab-CP versus CP alone was 0.61 (95% CI: 0.42–0.89; $p = .0090$; Fig. 2); median PFS in the two treatment groups was 6.9 months (95% CI: 6.1–8.3) and 5.9 months (95% CI: 4.2–6.5), respectively. In the subgroup analyses, improvement in PFS with bevacizumab-CP was evident in most patient subgroups assessed (Fig. 3).

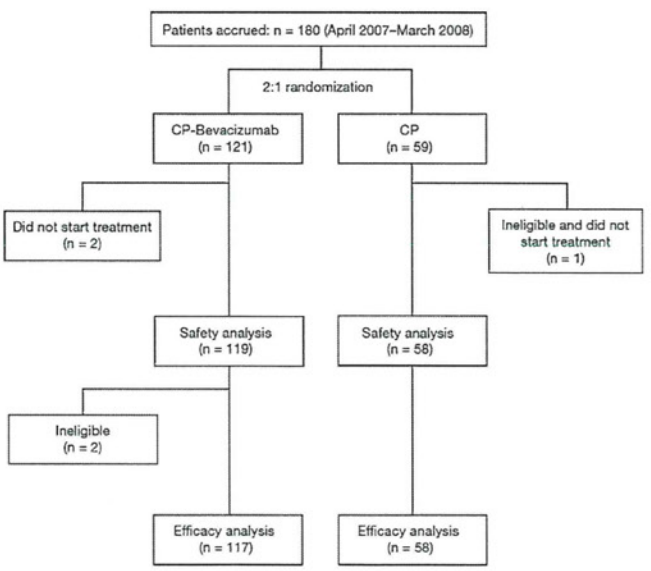

Fig. 1. Enrollment, randomization and follow-up of patients.

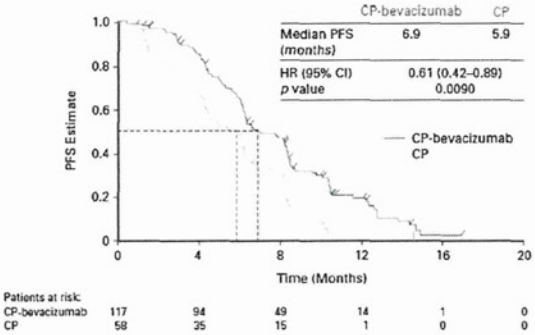

CP, carboplatin plus paclitaxel; PFS, progression-free survival; HR, hazard ratio.

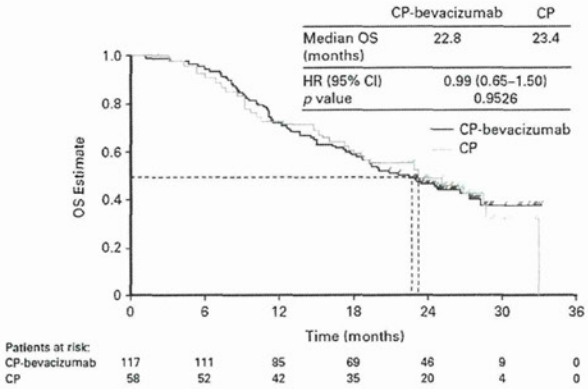

CP, carboplatin plus paclitaxel; OS, overall survival, HR, hazard ratio.

Fig. 2. Kaplan–Meier estimate of PFS and OS.

ORR was significantly higher with bevacizumab-CP than with CP alone (60.7% [95% CI: 51.2–69.6%] versus 31.0% [95% CI: 19.5–44.5%], respectively; $p = 0.0013$) (Table 2) as was the DCR (94.0% [95% CI: 88.1–97.6%] versus 70.7% [95% CI: 57.3–81.9%], $p = 0.0002$) (Table 2).

Table 2
Best tumor response in evaluable patients according to RECIST.

	CP ($n = 58$)	Bevacizumab-CP ($n = 117$)
CR, n (%)	0	1 (0.9%)
PR, n (%)	18 (31.0%)	70 (59.8%)
SD, n (%)	23 (39.7%)	39 (33.3%)
PD, n (%)	14 (24.1%)	5 (4.3%)
Non-evaluable, n (%)	3 (5.2%)	2 (1.7%)
ORR, % (95% CI)	31.0% (19.5–44.5)	60.7% (51.2–69.6)[a]
DCR, % (95% CI)	70.7% (57.3–81.9)	94.0% (88.1–97.6)[b]

CP, carboplatin plus paclitaxel; CR, complete response; PR, partial response; SD, stable disease; PD, progressive disease; ORR, objective response rate, DCR, disease control rate.

[a] $p = 0.0013$ versus CP (Cochran–Mantel–Haenszel test adjusted with the stratification factors used for randomization).

[b] $p = 0.0002$ versus CP (Cochran–Mantel–Haenszel test adjusted with the stratification factors used for randomization).

The median time to response was shorter with bevacizumab-CP (1.4 months; 95% CI: 1.4–1.5) than with CP alone (2.7 months; 95% CI: 1.4–2.8); however, this difference was not statistically significant (HR 1.45; 95% CI: 0.85–2.48; $p = 0.1496$). In addition, the median duration of response was longer in bevacizumab-CP recipients (6.9 months; 95% CI: 4.8–7.7) than in those treated with CP alone (5.6 months; 95% CI: 5.1–8.3), with an HR of 0.80 (95% CI: 0.43–1.48; $p = 0.4727$).

The HR for OS with bevacizumab-CP versus CP alone was 0.99 (95% CI: 0.65–1.50; $p = 0.9526$; Fig. 2). The median OS was 22.8 months (95% CI: 18.1–28.2) in the bevacizumab-CP group, compared with 23.4 months (95% CI: 17.4–28.5) in the CP alone group. Most patients in both treatment groups received post-study therapies (82% in bevacizumab-CP and 86% in CP alone). The number of patients who received third line therapy was higher in the CP alone group (48% in bevacizumab-CP and 57% in CP alone). EGFR-TKIs and docetaxel were the main drugs in second and third lines of therapy, administered to over 40% of patients (EGFR-TKIs: 41% and 47% in bevacizumab-CP and in CP alone, respectively; docetaxel: 42% and 40%) (Table 3).

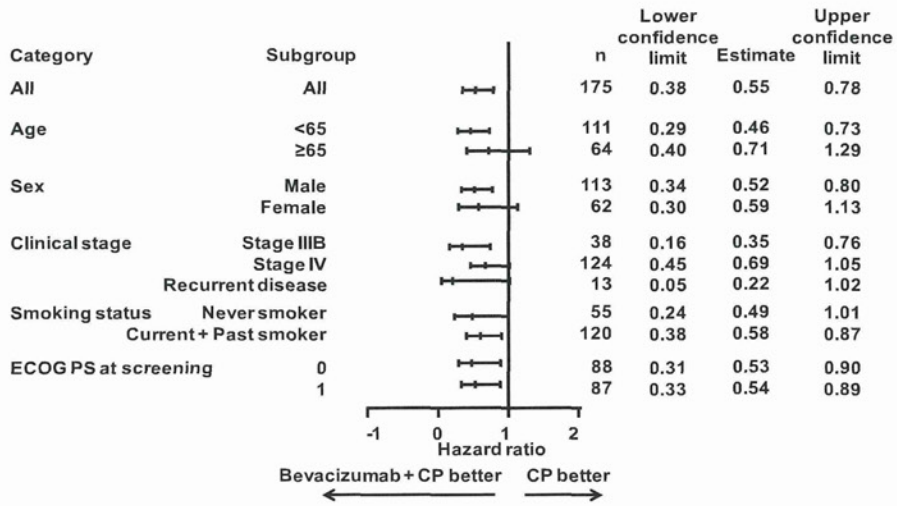

HR, hazard ratio; PFS, progression-free survival; CP, carboplatin plus paclitaxel; ECOG, Eastern Cooperative Oncology Group; PS, performance status.

Fig. 3. HRs (95% CI) for PFS, according to subgroup analysis.

Table 3
Post-protocol therapies (second line, third line).

Post-protocol therapy	CP ($n=58$)	Bevacizumab-CP ($n=117$)
Second line chemotherapy	86%	82%
Third line chemotherapy	57%	48%
Treatment		
docetaxel	40%	42%
EGFR-TKIs	47%	41%
gemcitabine	26%	24%
cisplatin	10%	9%
pemetrexed	5%	9%
investigational agent	17%	3%

CP, carboplatin plus paclitaxel; EFFR-TKIs, epidermal growth factor receptor inhibitors.

3.4. Safety analysis

Table 4 shows the incidences of AEs of special interest (i.e., AEs that have been associated with bevacizumab in combination with chemotherapy in previous studies) observed in both treatment groups.

Neutropenia was the most frequent AE of special interest in both treatment groups. Rates of any-grade proteinuria were higher in the bevacizumab treatment arm, but were generally mild-to-moderate in severity. Likewise, any-grade nasal bleeding occurred more frequently with bevacizumab-CP; however, no grade ≥3 events were reported.

While grade ≥3 hypertension was not reported in any patients treated with CP alone, it occurred in 11% of bevacizumab-CP recipients. No grade 4 hypertension was observed. Grade ≥3 leukopenia, neutropenia, and hyponatremia were modestly higher with bevacizumab-CP than with CP alone. Febrile neutropenia occurred in 8% of patients in the bevacizumab-CP group compared with 7% of patients in the CP alone group (Table 4).

Grade 1–2 hemoptysis was reported in 22% of patients treated with bevacizumab-CP compared with 5% of patients with CP alone. There were no grade 3 or 4 hemoptysis events; however, one grade 5 hemoptysis event was reported in a patient treated with bevacizumab-CP. This patient was male and had histology of adenocarcinoma with the primary tumor located in the left lower lobe and lymph-node metastases in the hilum of the left lung. The tumor did not have any cavitation. The patient had no complicating disease or any history of hemoptysis or bloody sputum and was not receiving anticoagulation therapy. The patient presented with grade 5 hemoptysis on day 12 of the second cycle.

Discontinuation of chemotherapy due to AEs occurred slightly more frequently in the bevacizumab-CP group (33% versus 26% of patients receiving CP alone). Twenty-six percent of patients discontinued bevacizumab because of an AE, mainly proteinuria, neutropenia, or hemoptysis.

3.5. Pharmacokinetic analysis

Pharmacokinetic parameters were analyzed in 51 patients who received bevacizumab-CP. Bevacizumab had a mean CL of 2.92 ± 0.56 mL/day/kg, a mean $t_{½}$ of 11.3 ± 2.1 days, a mean Vd of 46.51 ± 6.79 mL/kg, a mean AUC_{inf} of $5{,}314 \pm 1013$ μg day/mL and an MRT of 16.3 ± 3.0 days. The pharmacokinetic profile of bevacizumab in JO19907 was similar to that reported in patients treated with bevacizumab-CP in a US phase II study [10] (data not shown).

4. Discussion

In this phase II study, bevacizumab in combination with first-line CP in Japanese patients with non-squamous NSCLC reduced the hazard of disease progression by 39% (HR 0.61; 95% CI: 0.42–0.89). Furthermore, almost all evaluable patients who received bevacizumab achieved a tumor response or disease stabilization compared with only three-quarters of those who did not receive bevacizumab. This study was an open randomized trial and a potential bias could have been introduced by the use of non-blinded medication. Taking into consideration the nature of PFS as endpoint and non-placebo-controlled study design, tumor responses were evaluated by an Independent Review Committee in a blind manner.

Median PFS with bevacizumab-CP in JO19907 was 6.9 months, similar to that reported in phase III trials in Western populations (6.2 months with bevacizumab-CP [1] and 6.5–6.7 months with

Table 4
Selected adverse events of special interest associated with carboplatin-paclitaxel ± bevacizumab therapy.

Event	CP ($n=58$)			Bevacizumab-CP ($n=119$)		
	Grade 1/2	Grade 3	Grade 4	Grade 1/2	Grade 3	Grade 4
Hematologic toxicity						
Leukopenia	48%	40%	2%	44%	46%	4%
Neutropenia	9%	28%	57%	5%	18%	73%
Decreased hemoglobin	76%	3%	5%	73%	10%	2%
Thrombocytopenia	59%	3%	5%	67%	4%	<1%
Febrile neutropenia	–	7%	0	–	8%	0
Non-hematologic toxicity						
Hypertension	10%	0	0	37%	11%	0
Bleeding	31%	0	0	77%	<1%	0
Hemoptysis	5%	0	0	22%	0	0*
Nasal bleeding	12%	0	0	72%	0	0
Venous thromboembolism	0	3%	0	4%	0	0
Arterial thromboembolism	0	0	0	0	0	<1%
Congestive heart disease	2%	0	0	0	0	<1%
Proteinuria	17%	0	0	51%	<1%	0
Fatigue	53%	0	0	49%	3%	0
Vomiting	31%	0	0	34%	2%	0
Neuropathy	81%	5%	0	80%	8%	0
Muscle pain	71%	0	0	70%	0	0
Joint pain	79%	0	0	81%	<1%	0
Elevated AST	36%	0	0	44%	2%	<1%
Elevated ALT	36%	5%	0	44%	3%	<1%
Hyponatremia	3%	0	0	6%	7%	<1%
Treatment-related death			0%			<1%[a]

[a] One grade 5 hemoptysis event was reported in the bevacizumab group.
CP, carboplatin plus paclitaxel; AST, aspartate aminotransferase; ALT, alanine aminotransferase.

bevacizumab-cisplatin-gemcitabine [3]). The magnitude of reduction in the hazard of disease progression in this study with addition of bevacizumab to chemotherapy (HR 0.61) is also similar to, or greater than, that reported in the Western phase III studies (HR 0.66 in E4599 [1] and 0.75–0.82 in AVAiL [3]). Furthermore, subgroup analyses according to baseline patient characteristics indicated that bevacizumab was effective in most patient subgroups studied. This confirms the clinical activity of bevacizumab in Japanese patients with non-squamous NSCLC. Therefore, extrapolating the data from Western populations, bevacizumab could be considered as a first-line treatment option for Japanese patients presenting with non-squamous NSCLC.

No new safety signals were reported for bevacizumab in JO19907. The favorable tolerability profile of bevacizumab is reflected in the observation that 60.5% of patients were able to continue on bevacizumab monotherapy for a median of 6 cycles following chemotherapy. The incidences of grade ≥3 leukopenia, neutropenia, and hypertension were modestly higher in patients treated with bevacizumab; however, the majority of these events were controlled with standard clinical management. Grade 4 neutropenia occurred significantly more frequently with bevacizumab-CP than CP alone (73% versus 57%; $p = 0.0395$); however, there was no trend for an increased rate of febrile neutropenia or other infection in bevacizumab treated patients. Interestingly, the rate of grade 4 neutropenia in both groups was higher than that seen in the E4599 study (25.5% in bevacizumab-CP and 16.8% in CP alone) [1]. This supports the findings of Gandara et al., who reported that grade 4 neutropenia is more common in Japanese patients than Western patients treated with CP [8].

Although one grade 5 episode of hemoptysis did occur in the bevacizumab-CP group; overall hemoptysis events occurred at a rate similar to or lower than those reported in the E4599 and AVAiL studies, with all but one of these events grade 1 or 2 in severity. In addition to excluding patients with a history of hemoptysis, as in the E4599 study, the AVAiL and JO19907 studies excluded patients with tumors invading major blood vessels. Moreover, because retrospective analysis [11] of the E4599 study and another US phase II study [10] indicated that tumor cavitation is a potential risk factor for pulmonary hemorrhage in patients treated with bevacizumab plus chemotherapy, the eligibility criteria of this study also excluded patients with cavitated tumors. Appropriate selection of eligible patients might have made the risk of hemoptysis clinically manageable.

Unfortunately, the PFS improvement conferred by bevacizumab did not translate into an OS benefit in this study, which may be due to several limitations. Firstly, this study was not sufficiently powered to assess the OS benefit of bevacizumab plus CP, which was a secondary endpoint. Also, the median survival times were >22 months in both arms, approximately double the median survival time observed in the E4599 study, which undoubtedly reflects the unexpectedly long post-progression survival (PPS) [12] due to the efficacy of post-protocol therapies. It has been reported that when PPS is long, statistical power to detect a difference in OS is greatly reduced and that lack of statistically significant difference in OS does not imply lack of OS benefit [13]. In our trial, more than 80% of the patients received subsequent therapies, compared with less than 50% in E4599. Moreover, many newly developed efficacious drugs with proven survival benefit, such as EGFR-TKIs or docetaxel, were used in the post-study period. Taking into consideration the higher frequency of EGFR mutations in Japanese patients, especially, use of EGFR-TKIs could contribute to the prolonged PPS. Thus, our second limitation is that we were unable to thoroughly collect and report information on the second- or third-line therapies used in this trial, including treatment duration and tumor responses to those post-protocol therapies. In addition, neither investigation nor report of the EGFR mutation status was not required in this trial. More detailed analyses on post-protocol therapies might be necessary to evaluate the OS benefit in future study reports.

In conclusion, addition of bevacizumab to first-line CP results in similar PFS benefits in Japanese patients with advanced non-squamous NSCLC as in Western patients. No new safety concerns were raised in Japanese population.

Conflict of interest statement

Hideo Kunitoh received honoraria from Bristol-Myers Squibb and Chugai pharmaceuticals and served as an advisor to Chugai pharmaceuticals. Yukito Ichinose, Nobuyuki Yamamoto and Katsuyuki Kiura received honoraria from Chugai pharmaceuticals. Kazuhiko Nakagawa received honoraria from Bristol-Myers Squibb and Chugai pharmaceuticals. Shunichi Negoro received honoraria from Bristol-Myers Squibb and Chugai pharmaceuticals. Masahiro Fukuoka received honoraria from AstraZeneca, Boehringer Ingelheim and Chugai pharmaceuticals.

Acknowledgements

This study was sponsored by Chugai Pharmaceuticals, and, support for third party writing assistance for this manuscript was provided by Chugai Pharmaceuticals.

References

[1] Sandler A, Gray R, Perry MC, Brahmer J, Schiller JH, Dowlati A, et al. Paclitaxel-carboplatin alone or with bevacizumab for non-small-cell lung cancer. N Engl J Med 2006;355:2542–50.
[2] Schiller JH, Harrington D, Belani CP, Langer C, Sandler A, Krook J, et al. Comparison of four chemotherapy regimens for advanced non-small-cell lung cancer. N Engl J Med 2002;346:92–8.
[3] Reck M, von Pawel J, Zatloukal P, Ramlau R, Gorbounova V, Hirsh V, et al. Phase III trial of cisplatin plus gemcitabine with either placebo or bevacizumab as first-line therapy for nonsquamous non-small-cell lung cancer: AVAiL. J Clin Oncol 2009;27:1227–34.
[4] Shepherd FA, Rodrigues Pereira J, Ciuleanu T, Tan EH, Hirsh V, Thongprasert S, et al. Erlotinib in previously treated non-small-cell lung cancer. N Engl J Med 2005;353:123–32.
[5] Thatcher N, Chang A, Parikh P, Rodrigues Pereira J, Ciuleanu T, von Pawel J, et al. Gefitinib plus best supportive care in previously treated patients with refractory advanced non-small-cell lung cancer: results from a randomised, placebo-controlled, multicentre study (Iressa Survival Evaluation in Lung Cancer). Lancet 2005;366:1527–37.
[6] Mitsudomi T, Morita S, Yatabe Y, Negoro S, Okamoto I, Tsurutani J, et al. Gefitinib versus cisplatin plus docetaxel in patients with non-small-cell lung cancer harbouring mutations of the epidermal growth factor receptor (WJTOG3405): an open label, randomised phase 3 trial. Lancet Oncl 2010;11:121–8.
[7] Maemondo M, Inoue A, Kobayashi K, Sugawara S, Oizumi S, Isobe H, et al. Gefitinib or chemotherapy for non-small-cell lung cancer with mutated EGFR. N Engl J Med 2010;362:2380–8.
[8] Gandara DR, Kawaguchi T, Crowley J, Moon J, Furuse K, Kawahara M, et al. Japanese-US common-arm analysis of paclitaxel plus carboplatin in advanced non-small-cell lung cancer: a model for assessing population-related pharmacogenomics. J Clin Oncol 2009;27:3540–6.
[9] Therasse P, Arbuck SG, Eisenhauer EA, Wanders J, Kaplan RS, Rubinstein L, et al. New guidelines to evaluate the response to treatment in solid tumors. European Organization for Research and Treatment of Cancer, National Cancer Institute of the United States, National Cancer Institute of Canada. J Natl Cancer Inst 2000;92:205–16.
[10] Johnson DH, Fehrenbacher L, Novotny WF, Herbst RS, Nemunaitis JJ, Jablons DM, et al. Randomized phase II trial comparing bevacizumab plus carboplatin and paclitaxel with carboplatin and paclitaxel alone in previously untreated locally advanced or metastatic non-small-cell lung cancer. J Clin Oncol 2004;22:2184–91.
[11] Sandler AB, Schiller JH, Gray R, Dimery I, Brahmer J, Samant M, et al. Retrospective evaluation of the clinical and radiographic risk factors associated with severe pulmonary hemorrhage in first-line advanced, unresectable non-small-cell lung cancer treated with carboplatin and paclitaxel plus bevacizumab. J Clin Oncol 2009;27:1405–12.
[12] Saad ED, Katz A, Buyse M. Overall survival and post-progression survival in advanced breast cancer: a review of recent randomized clinical trials. J Clin Oncol 2010;28:1958–62.
[13] Broglio KR, Berry DA. Detecting an overall survival benefit that is derived from progression-free survival. J Natl Cancer Inst 2009;101:1642–9.